an alternative regulator of *MYC* in human GBM. Distinct from the p53-MYC regulatory mechanism, TAp63 is activated in response to TMZ-induced stress, and does not bind to intron 2 but is recruited onto the upstream promoter region of *MYC* to directly repress transcription. In addition, the interaction between the p53 and MYC signaling networks are important for cellular proliferation and differentiation in the prevention of GBM pathogenesis[14,15,17]. However p53 is functionally inactivated in many aggressive GBMs[12]. Therefore, the newly identified TAp63-*MYC* regulatory pathway may serve as an alternative activator of the p53-regulated tumour suppressive pathways[10,21,25,26].

Recently, there have been several reports on the role of p53 in TMZ resistance in GBM. TMZ activates p53 to induce apoptosis in GBM cells[27,28], and functional inactivation of the p53 pathway by overexpression of the α5β1 integrin contributes to TMZ resistance in high-grade glioma[27]. On the other hand, reports also suggest that p53 inactivation rather increases TMZ sensitivity in GBM cell lines[29] and *in vivo* xenograft models[30], and that the status of p53 is not a molecular predictor of the response to chemotherapy with TMZ[31]. These discrepancies indicate the existence of an alternative mechanism underlying TMZ resistance in GBM which is independent of the p53 status. Our present data show that the TAp63-*MYC* pathway contributes to TMZ sensitivity in both *p53*-wild type and -mutant GBM cells, and that the expression levels of *TAp63* and *MYC* are prognostic factors in TMZ-treated GBM.

In conclusion, our results clearly indicate that *MYC* is a novel TAp63 target gene and that the TAp63-*MYC* pathway has a crucial role in mediating suppression of GBM progression. Pharmacological targeting of the TAp63-*MYC* pathway may therefore provide new rational therapeutic strategies against TMZ-resistant GBMs.

Methods

Glioma tumour samples and tissue dissection. A total of 89 malignant glioma samples comprising of newly-diagnosed GBM (World Health Organization (WHO) grade 4, n = 59), newly-diagnosed anaplastic astrocytoma (WHO grade 3, n = 7), newly-diagnosed anaplastic oligoastrocytoma (WHO grade 3, n = 3) and 20 recurrent malignant gliomas (17 GBMs, 3 anaplastic oligoastrocytomas) were collected between 1994 and 2011 and obtained from the Chiba Cancer Center upon receiving informed consent under an institutional review board-approved protocol. The present project was approved by the Ethics Committee of the Faculty of Biology and Medicine at the Chiba Cancer Center (protocol 15–19). After surgery, the patients were treated according to previously described protocols[32]. Although procarbazine, ACNU and vincristine (PAV) were used for chemotherapy until 2006, TMZ was used from 2006 in our facility. The tumour samples were routinely processed using a BenchMark® XT automated slide-processing system (Ventana Medical Systems, USA) for optimization and performance evaluation of the immunohistochemical assay for p63 protein. Paraffin-embedded tissue sections on glass slides were baked prior to the deparaffinization step with EZ Prep™ (Ventana). The sections were then washed with a mixture of Immunoblock (Dainippon Sumitomo Pharma Co.) and reaction buffer, followed by incubation with a mouse anti-human p63 monoclonal antibody (clone 4A4, Dako). The tumour samples were divided into three specimens: immediately snap-frozen in liquid nitrogen; diagnostic frozen sections for the Department of Pathology; and formalin-fixed paraffin-embedded sections. The specimens were homogenised using a rotor/stator homogenizer. DNA and RNA were extracted from the patient samples as previously described[33]. Total RNA was extracted from three healthy human brain tissue samples purchased from separate sources, Clontech, Stratagene and Zyagen, and the highest p63-expressing sample was used as the threshold standard. A newly diagnosed GBM specimen (supplied by Chiba Cancer Center) was used to generate cancer tissue-originated spheroid cultures as described previously[19].

Cell lines and specimen collection. GBM cell lines were purchased from the American Type Culture Collection (U87MG) and Health Science Research Resources Bank (YH-13, KNS-42 and SF126). The cell lines were cultured in modified Eagle's medium containing 20% (YH-13), 5% (KNS42) or 10% (U87MG and SF126) heat-inactivated foetal bovine serum (Invitrogen).

Temozolomide (TMZ) treatment. TMZ was purchased from LKT Laboratories Inc., and freshly prepared for experimental use. TMZ was added at the final concentrations 24 h after cell seeding for each experiment.

RT-PCR and qRT-PCR. The primers are described in the *SI Methods.*

Gene knockdown assay. The following gene-specific siRNAs were purchased: siTAp63-1, sense 5′-CAGCUAUAUGUUCAGUUCTT-3′ and antisense 5′-GAA CUGAACAUAUAGCUGTT-3′; siTAp63-3, sense 5′-CAGAAGAUGGUGCG ACAAATT-3′ and antisense 5′-UUUGUCGCACCAUCUUCUGTT-3′ from Sigma; siMyc-26 for CGAUGUUGUUUCUGUGGAA and siMyc-29 for CUACCAGGC UGCGCGCAAA from Thermo Scientific. The control siRNA (Mission siRNA Universal Negative Control SIC-001) was purchased from Sigma. All transfections were performed using Lipofectamine™ RNAiMax (Invitrogen). The transfections were carried out twice, with reverse transfection immediately following cell count to 1 × 10^5 cells/ml and forward transfection 24 h after reverse transfection.

Overexpression of TAp63 in human GBM cells. *TAp63α* was fused to the FLAG epitope at the NH_2 terminus and cloned into the lentiviral pHR vector. The lentivirus was produced by cotransfecting pHR, pCMVR and pMDG plasmids into HEK293T cells using the FuGENE HD reagent (Roche). At 12 and 24 h after transfection, the viral supernatants were collected and mixed with GBM cells.

Western blot assay. We resolved cell proteins by SDS-PAGE prior to electroblotting onto a PVDF membrane. We incubated the membranes with the following primary antibodies overnight: anti-p63 (4A4) (1 : 1000; sc-8431, Santa Cruz Biotechnology), anti-Myc (N-262) (1 : 2000; sc-764, Santa Cruz Biotechnology, Santa Cruz, CA, USA), and anti-Actin (20-33) (1 : 4000; A5060, Sigma). The membranes were then incubated with a horseradish peroxidase-conjugated secondary antibody (anti-rabbit IgG #7074, 1 : 2000–1 : 4000 or anti-mouse IgG #7076, 1 : 2000; Cell Signaling Technology) and the bound proteins were visualized using a chemiluminescence-based detection kit (ECL and ECL pro kit; Amersham and PerkinElmer).

Chromatin immunoprecipitation (ChIP) assay. YH-13 cells transfected with siRNA or exposed to TMZ at increasing concentrations between 150–300 μM were harvested 24 h after the second transfection or after TMZ exposure. ChIP assays were performed with a ChIP assay kit (Millipore) according to the manufacturer's instructions using an anti-p63 antibody (clone (4A4) sc-8431, Santa Cruz Biotechnology) and normal mouse IgG (015-000-003, Jackson ImmunoResearch Laboratories Inc.). The primer sequences for the *MYC* promoter are described in the *SI Methods.*

Luciferase reporter assay. pBV-LUC Del1 (#16601) and Del2 (#16602) containing the *MYC* promoter regions at nucleotides −2268 to +525 and −1061 to +525 from the transcription start site, respectively, were obtained from Addgene. YH-13 and U87MG cells were seeded at 5 × 10^4 cells/well in a 24-well plate and allowed to adhere overnight. The cells were subjected to lentiviral infection on the following day with control pHR vector or pHR-*TAp63α* vector. At 54 h after infection, the cells were seeded in triplicate on 12-well plates at 1 × 10^5 cells/well and cultured for 24 h. They were then cotransfected with 400 ng of *MYC* luciferase reporter construct and 40 ng of *Renilla* TK with Lipofectamine 2000 (Invitrogen). At 18 h after the second transfection, the cells were harvested and the luciferase activity was determined using a dual-luciferase assay system (Promega) according to the manufacturer's instructions.

Migration and invasion assay. The invasive potential of GBM cells *in vitro* was measured by evaluating the number of invading cells using Matrigel-coated Transwell inserts (BD Biosciences) according to the manufacturer's instructions. YH-13 and U87MG cells transfected with siTAp63 and siMyc were seeded onto an insert with 8 μm pores (BD Biosciences) in a 24-well plate at 2 × 10^5 cells/ml. The cells were treated with 150 μM TMZ and counted 18 h after siRNA knockdown. Cells on the lower side of the membrane were fixed with 4% paraformaldehyde and stained using a Diff Quick Staining Kit (Sysmex).

Cell viability assay (MTT assay). Cell viability was quantified by the 3-(4, 5-dimethylthiazol-2-yl)-2, 5-diphenyltetrazolium bromide (MTT) method. Cells were collected and seeded in 96-well plates at 1 × 10^5 cells/well. After addition of 10 μl of MTT tetrazolium salt (Sigma) solution to each well, the plates were incubated in a CO_2 incubator. The absorbance of each well was measured using a Dynatech MR5000 plate reader with a test wavelength of 450 nm and a reference wavelength of 630 nm.

Sphere formation assay. We evaluated neurospheres derived from YH-13 cells transfected with the appropriate siRNA. After performing cell counts, we plated single cells in 60 mm non-coated dishes (2.5 × 10^5 cells/dish; Iwaki) to check the sphere morphology, and used a 96-well ultra-low cluster plate (2.5 × 10^4 cells/well; Costar) to count the spheres. The cells were allowed to proliferate in serum-free DMEM (Sigma) and F12 medium (Invitrogen) containing epidermal growth factor (Sigma) and 20 ng/ml basic fibroblast growth factor (Invitrogen) with 2% B27 supplement (Invitrogen). Half of the medium was replaced with fresh culture medium every 7 days.

Mouse xenograft models. Six- or seven-week-old male athymic BALB/c nu/nu mice were obtained from Japan SLC, Inc. The mice were anesthetized with intraperitoneal tribromoethanol (Wako) at 20 mg/kg body weight. U87MG cells mixed with an equal volume of Matrigel were implanted into the right and left hind legs. One week after tumour cell implantation, we injected 50 μl of Atelogene (Koken) with either control siRNA or siTAp63 (10 μM) into the U87MG xenografts. A total of 15 mg/kg TMZ in PBS was administered intraperitoneally once per week. Tumour growth was

measured with calipers and calculated by the formula: volume (V) = length (A) × width (B) × width (B) × 0.5. These studies were approved by the Committee for Animal Care at the Chiba Cancer Center Research Institute.

Statistical analysis. Data is presented as the mean ± the standard deviation. Statistical significances in the clinical data were calculated using Kaplan-Meier survival curves. Statistical analyses were performed with JMP® 10 (SAS institute Japan).

1. Chen, J., McKay, R. M. & Parada, L. F. Malignant glioma: lessons from genomics, mouse models, and stem cells. *Cell* **149**, 36–47 (2012).
2. Mrugala, M. M. & Chamberlain, M. C. Mechanisms of disease: temozolomide and glioblastoma - look to the future. *Nat. Clin. Pract. Oncol.* **5**, 476–486 (2008).
3. Stupp, R. *et al.* Radiotherapy plus concomitant and adjuvant temozolomide for glioblastoma. *N. Engl. J. Med.* **352**, 987–996 (2005).
4. Hegi, M. E. *et al.* MGMT gene silencing and benefit from temozolomide in glioblastoma. *N. Engl. J. Med.* **352**, 997–1003 (2005).
5. Shah, N. *et al.* Comprehensive analysis of *MGMT* promoter methylation: correlation with MGMT expression and clinical response in GBM. *PLoS One* **6**, e16146 (2011).
6. Beier, D., Schulz, J. B. & Beier, C. P. Chemoresistance of glioblastoma cancer stem cells - much more complex than expected. *Mol. Cancer* **10**, 128 (2011).
7. Osada, M. *et al.* Cloning and functional analysis of human p51, which structurally and functionally resembles p53. *Nat. Med.* **4**, 839–843 (1998).
8. Yang, A. *et al.* p63, a p53 homolog at 3q27-29, encodes multiple products with transactivating, death-inducing, and dominant-negative activities. *Mol. Cell* **2**, 305–316 (1998).
9. Kaghad, M. *et al.* Monoallelically expressed gene related to p53 at 1p36, a region frequently deleted in neuroblastoma and other human cancers. *Cell* **90**, 809–819 (1997).
10. Stiewe, T. The p53 family in differentiation and tumorigenesis. *Nat. Rev. Cancer* **7**, 165–168 (2007).
11. Deyoung, M. P. & Ellisen, L. W. p63 and p73 in human cancer: defining the network. *Oncogene* **26**, 5169–5183 (2007).
12. Cancer Genome Atlas Research Network. Comprehensive genomic characterization defines human glioblastoma genes and core pathways. *Nature* **455**, 1061–1068 (2008).
13. Suenaga, Y. *et al.* TATA-binding protein (TBP)-like protein is engaged in etoposide-induced apoptosis through transcriptional activation of human TAp63 gene. *J. Biol. Chem.* **284**, 35433–35440 (2009).
14. Aguda, B. D., Kim, Y., Kim, H. S., Friedman, A. & Fine, H. A. Qualitative network modeling of the Myc-p53 control system of cell proliferation and differentiation. *Biophys. J.* **101**, 2082–2091 (2011).
15. Bredel, M. *et al.* Functional network analysis reveals extended gliomagenesis pathway maps and three novel MYC-interacting genes in human gliomas. *Cancer Res.* **65**, 8679–8689 (2005).
16. Zheng, H. *et al.* p53 and Pten control neural and glioma stem/progenitor cell renewal and differentiation. *Nature* **455**, 1129–1133 (2008).
17. Ho, J. S., Ma, W., Mao, D. Y. & Benchimol, S. p53-dependent transcriptional repression of c-myc is required for G1 cell cycle arrest. *Mol. Cell Biol.* **25**, 7423–7431 (2005).
18. Krieg, A. J., Hammond, E. M. & Giaccia, A. J. Functional analysis of p53 binding under differential stresses. *Mol. Cell Biol.* **26**, 7030–7045 (2006).
19. Kondo, J. *et al.* Retaining cell-cell contact enables preparation and culture of spheroids composed of pure primary cancer cells from colorectal cancer. *Proc. Natl. Acad. Sci. USA* **108**, 6235–6240 (2011).
20. Wang, J. *et al.* c-Myc is required for maintenance of glioma cancer stem cells. *PLoS One* **3**, e3769 (2008).
21. Su, X. *et al.* TAp63 suppresses metastasis through coordinate regulation of Dicer and miRNAs. *Nature* **467**, 986–990 (2010).
22. Melino, G. p63 is a suppressor of tumorigenesis and metastasis interacting with mutant p53. *Cell Death Differ.* **18**, 1487–1499 (2011).
23. Kim, S., Han, J., Kim, J. & Park, C. Maspin expression is transactivated by p63 and is critical for the modulation of lung cancer progression. *Cancer Res.* **64**, 6900–6905 (2004).
24. Adorno, M. *et al.* A Mutant-p53/Smad complex opposes p63 to empower TGFβ-induced metastasis. *Cell* **137**, 87–98 (2009).
25. Sachdeva, M. *et al.* p53 represses c-Myc through induction of the tumor suppressor miR-145. *Proc. Natl. Acad. Sci. USA* **106**, 3207–3212 (2009).
26. Guo, X. *et al.* TAp63 induces senescence and suppresses tumorigenesis *in vivo*. *Nat. Cell Biol.* **11**, 1451–1457 (2009).
27. Janouskova, H. *et al.* Integrin α5β1 plays a critical role in resistance to temozolomide by interfering with the p53 pathway in high-grade glioma. *Cancer Res.* **72**, 3463–3470 (2012).
28. Zhang, W. B. *et al.* Activation of AMP-activated protein kinase by temozolomide contributes to apoptosis in glioblastoma cells via p53 activation and mTORC1 inhibition. *J. Biol. Chem.* **285**, 40461–40471 (2010).
29. Blough, M. D. *et al.* Effect of aberrant p53 function on temozolomide sensitivity of glioma cell lines and brain tumor initiating cells from glioblastoma. *J. Neurooncol.* **102**, 1–7 (2011).
30. Dinca, E. B. *et al.* p53 small-molecule inhibitor enhances temozolomide cytotoxic activity against intracranial glioblastoma xenografts. *Cancer Res.* **68**, 10034–10039 (2008).
31. Weller, M. *et al.* Molecular predictors of progression-free and overall survival in patients with newly diagnosed glioblastoma: a prospective translational study of the German Glioma Network. *J. Clin. Oncol.* **27**, 5743-5750 (2009).
32. Iuchi, T. *et al.* Hypofractionated high-dose irradiation for the treatment of malignant astrocytomas using simultaneous integrated boost technique by IMRT. *Int. J. Radiat. Oncol. Biol. Phys.* **64**, 1317–1324 (2006).
33. Ohira, M. *et al.* Expression profiling using a tumor-specific cDNA microarray predicts the prognosis of intermediate risk neuroblastomas. *Cancer Cell* **7**, 337–350 (2005).

Acknowledgments

We would like to thank R. I. Selim, Y. Kaneko, D. Matsumoto and K. Ando for technical support, A. Sada and N. Kitabayashi for DNA and RNA extractions, Y. Nakamura for sequencing support, R. Takano for lentivirally expressed TAp63α, and E. Isogai for helpful discussions and experimental assistance with mice throughout the course of this study. This work was supported in part by a grant-in-aid from the Ministry of Health, Labour and Welfare for the Third Term Comprehensive Control Research for Cancer, Japan, and a grant-in-aid for Scientific Research on Priority Areas from the Ministry of Education, Culture, Sports, Science and Technology, Japan.

Author contributions

T.Y. and Y.S. designed, performed and analysed cellular and animal experiments and wrote the manuscript. T.I. collected clinical samples and analysed clinical data. J.A. and A.T. performed and analysed cellular and animal experiments and wrote the manuscript. M.I. and A.A. performed pathological analyses of surgical tissue samples. M.O. assisted with figures and experimental design. M.I. supported the generation of cancer tissue originated-spheroid cultures. H.K. and S.Y. performed genomic mutation search experiments. N.S. assisted in experiments and associated clinical annotations. A.N. designed and supervised the experiments, analysed data, and wrote and edited the manuscript.

Additional information

Supplementary information accompanies this paper at http://www.nature.com/scientificreports

Competing financial interests: The authors declare no competing financial interests.

How to cite this article: Yamaki, T. *et al.* Temozolomide suppresses *MYC* via activation of TAp63 to inhibit progression of human glioblastoma. *Sci. Rep.* **3**, 1160; DOI:10.1038/srep01160 (2013).

Brain Tumor Pathol
DOI 10.1007/s10014-012-0119-8

ORIGINAL ARTICLE

Clinical and histological characteristics of recurrent oligodendroglial tumors: comparison between primary and recurrent tumors in 18 cases

Masayuki Kanamori · Toshihiro Kumabe · Ichiyo Shibahara · Ryuta Saito · Yoji Yamashita · Yukihiko Sonoda · Hiroyoshi Suzuki · Mika Watanabe · Teiji Tominaga

Received: 29 May 2012 / Accepted: 17 September 2012

Abstract Changes in histological and genetic characteristics were investigated in 18 paired primary and recurrent oligodendroglial tumors, using sequencing analysis for isocitrate dehydrogenase (IDH) 1 and 2 gene mutation, Ki-67 and p53 immunohistochemistry, and fluorescent in situ hybridization for loss of heterozygosity of chromosomes 1p and 19q (1p/19q co-deletion). Malignant transformation occurred in 5 of 8 cases with World Health Organization (WHO) grade II tumors, but in 0 of 10 cases with WHO grade III tumors progressing to glioblastoma. Thirteen of the 18 cases carried IDH1 gene mutation. Tumors with IDH1 mutation tended to survive for longer, even after recurrence, but newly developed microvascular proliferation, tumor necrosis, and elevated Ki-67 labeling index were common. Eleven of the 13 IDH1-mutation tumors had either 1p/19q co-deletion or nuclear expression of p53, but all 5 IDH1/2 wild-type tumors had neither. All cases had the same profile for 1p/19q status at recurrence, but nuclear expression of p53 changed from negative to positive in 2 of 6 cases with IDH1 mutation and 1p/19q co-deletion. WHO grade II oligodendroglial tumors show a high rate of malignant transformation, possibly involving p53 in tumors with IDH1 mutation and 1p/19q co-deletion. Tumors with IDH1 mutation had a more aggressive histological phenotype despite their better prognosis.

Keywords Recurrent oligodendroglial tumor · IDH1/2 gene · p53 · 1p/19q co-deletion · Ki-67 labeling index

M. Kanamori · T. Kumabe (✉) · I. Shibahara · R. Saito · Y. Yamashita · Y. Sonoda · T. Tominaga
Department of Neurosurgery, Tohoku University Graduate School of Medicine, 1-1 Seiryo-machi, Aoba-ku, Sendai 980-8574, Japan
e-mail: kuma@nsg.med.tohoku.ac.jp

H. Suzuki
Department of Pathology and Laboratory Medicine, Sendai Medical Center, Sendai, Japan

M. Watanabe
Department of Pathology, Tohoku University Hospital, Sendai, Japan

Introduction

Oligodendroglial tumors, including oligodendroglioma (OD), oligoastrocytoma (OA), anaplastic oligodendroglioma (AOD), and anaplastic oligoastrocytoma (AOA), account for 6.8 % of all cases of glial tumors in Japan [1]. These entities have better prognoses than astrocytic tumors, but most patients ultimately experience disease progression. The changes in histological diagnosis for the 95 cases treated prospectively in the North Central Cancer Treatment Group study were recently reported [2]. The World Health Organization (WHO) grade increased after recurrence in 51 % of all cases, in 57 % of WHO grade II tumors, and in 13 % of WHO grade III tumors. Additionally, significant changes occurred in the diagnosis of recurrent tumor to pure astrocytic, pure oligodendroglial, and mixed tumor [2]. Therefore, dynamic changes could occur in the histological character of recurrent oligodendroglial tumors.

Changes in genetic aberrations at progression have also been demonstrated. For example, p16 deletions, gain of chromosome 7, and loss of chromosome 10 are considered to be associated with progression [2–4]. Recently, somatic mutations in the isocitrate dehydrogenase 1 (IDH1) gene or IDH2 gene have been found in adult astrocytomas or ODs [5–7]. Oligodendroglial tumors with IDH1 or IDH2

Published online: 02 October 2012

mutations have better prognosis [8–10], and express mutually exclusive loss of heterozygosity of chromosomes 1p and 19q (1p/19q co-deletion) or p53 mutations [11]. In contrast, IDH1/2 wild-type tumors have poor prognosis and show no 1p/19q co-deletion. The mechanisms of these histological changes—or how these representative genetic aberrations are associated with tumor progression in IDH1 or IDH2 mutated and wild-type recurrent oligodendroglial tumors—remain unclear.

The present study retrospectively reviewed the clinical and histological findings of recurrent oligodendroglial tumors to clarify the dynamic changes in all recurrent oligodendroglial tumors, and analyzed the histological and genetic characteristics of recurrent tumors with IDH1 or IDH2 mutations, those with IDH1/2 wild-type genes, and those with 1p/19q co-deleted or retained.

Materials and methods

Patients

Our facility treated 123 patients with histologically verified oligodendroglial tumors between April 1978 and July 2011. The histological diagnosis was established by two neuropathologists (H.S. and M.W.) using current WHO criteria [12]. However, the definitive criteria for glioblastoma with oligodendroglial component (GBMO) remains to be established at this point. In this series, the criteria for GBMO were as follows: the tumor was composed of typical glioblastoma, including marked atypia, high cellularity, pseudopalisading or large necrosis, microvascular proliferation, and an oligodendroglial component. AOA with a small area of tumor necrosis was excluded from GBMO. During this period, 36 patients had recurrent disease, 18 of whom underwent salvage surgery. We reviewed the histological findings of the primary and recurrent tumors. This study was approved by the institutional ethics committee of Tohoku University Graduate School of Medicine, in accordance with the Declaration of Helsinki. Informed consent for molecular and histological analyses of the specimens was obtained from all patients involved in this study.

Analysis of IDH1 and IDH2 gene mutations

Analysis of IDH1 and IDH2 gene mutations was performed as described previously [7]. Genomic deoxyribonucleic acid (DNA) was extracted from snap-frozen tissues, and the DNA fragments including codon 132 of the IDH1 gene and codon 172 of the IDH2 gene were amplified. Direct sequencing analysis of the purified polymerase chain reaction product was performed in an automated DNA analyzer (CEQ 8000; Beckman Coulter, Brea, CA, USA).

Immunohistochemical analysis and fluorescent in situ hybridization (FISH)

Immunohistochemical and FISH analysis was performed as described previously [13]. For immunohistochemical analysis, formalin-fixed, paraffin-embedded tissues were cut into 2 μm thick paraffin sections. The primary antibodies were mouse monoclonal antibody for p53 (Nichirei, Tokyo, Japan; not diluted), and Ki-67 (DAKO, Glostrup, Denmark; 1:300). The cut-off value of the labeling index was 10 % for p53 staining. The Ki-67 labeling index was quantified by counting the number of positive cells among 1000 cells in the regions with the most immunoreactivity. For the FISH analysis of 1p/19q co-deletion, 2 μm thick paraffin-embedded sections were deparaffinized and hybridized with locus-specific probes for 19q13 (SpectrumOrange; Abbott Molecular, Des Plaines, IL, USA), 19p13 (SpectrumGreen; Abbott Molecular), 1p36 (SpectrumOrange), and 1q25 (SpectrumGreen). Nuclei were counterstained with 4′,6-diamino-2-phenylindole and mounted in antifade solution.

Statistical analysis

Continuous variables were compared with Student's *t* test, and categorical variables were compared with the chi-squared test or Fisher's exact test. Kaplan–Meier curves were generated for the progression-free survival rate after initial surgery and the overall survival rate after recurrence. We compared curves for the two groups with the log-rank test. A probability value of less than 0.05 was considered statistically significant. All statistical analyses were performed with Dr. SPSS (SPSS, Chicago, IL, USA).

Results

Demographics of the cases with recurrent oligodendroglial tumors

The 13 male and 5 female patients were aged 29–78 (median 50.5) years at initial treatment. The intervals between surgeries for primary and recurrent tumors ranged from 1 to 234 (median 28) months. For histological diagnosis, debulking surgery was performed in 15 cases and biopsy in 3. The histological diagnosis of primary tumors was OD in 6, OA in 2, AOD in 6, and AOA in 4 (Fig. 1). The strategies for postoperative treatment were described previously [13]. Postoperatively, only radiation therapy was performed in 5 patients, only chemotherapy in 1, a combination of radiation and chemotherapy in 9, and no additional treatment in 3. Radiation therapy consisted of 1.2 Gy twice daily for a total of 72 Gy in 60 fractions to the tumor bed for AOD and AOA, and 2.0 Gy once daily

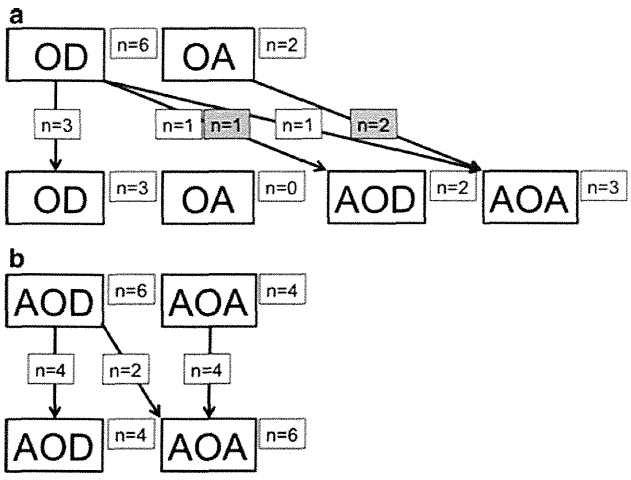

Fig. 1 Changes in the histological diagnoses of primary (*upper row*) and recurrent (*lower row*) oligodendroglial tumors among WHO grade II tumors (**a**) and WHO grade III tumors (**b**). The cases who did not receive any adjuvant therapy are indicated in *gray*. *OD* oligodendroglioma, *OA* oligoastrocytoma, *AOD* anaplastic oligodendroglioma, *AOA* anaplastic oligoastrocytoma

for a total of 60 Gy in 30 fractions for OD and OA. Chemotherapy consisted of nimustine hydrochloride (ACNU) in 7 patients, combination chemotherapy of procarbazine, ACNU, and vincristine in 2, and temozolomide in 1.

The histological diagnosis of the recurrent tumors was OD in 3 cases, AOD in 6, and AOA in 9 (Fig. 1). As radiation may induce cellular atypia, astrocytoma-like morphology in oligodendroglioma, and endothelial cell atypia mimicking microvascular proliferation [20], we diagnosed a malignant transformation when newly developed glomeruloid or epithelioid microvascular proliferation or brisk mitosis (>6 mitosis/10 high power fields) was found. Malignant transformation occurred in 5 of 8 cases (63 %) with WHO grade II tumors (Fig. 1a). These 5 cases had newly developed definitive microvascular proliferation. All of the cases had brisk mitosis. The changes in the histological diagnosis of primary and recurrent tumors were OD to AOD in 2 cases, OD to AOA in 1, and OA to AOA in 2 (Fig. 1a). Initial treatment after surgery was no treatment in 3 cases (Fig. 2) and only radiation therapy in 2

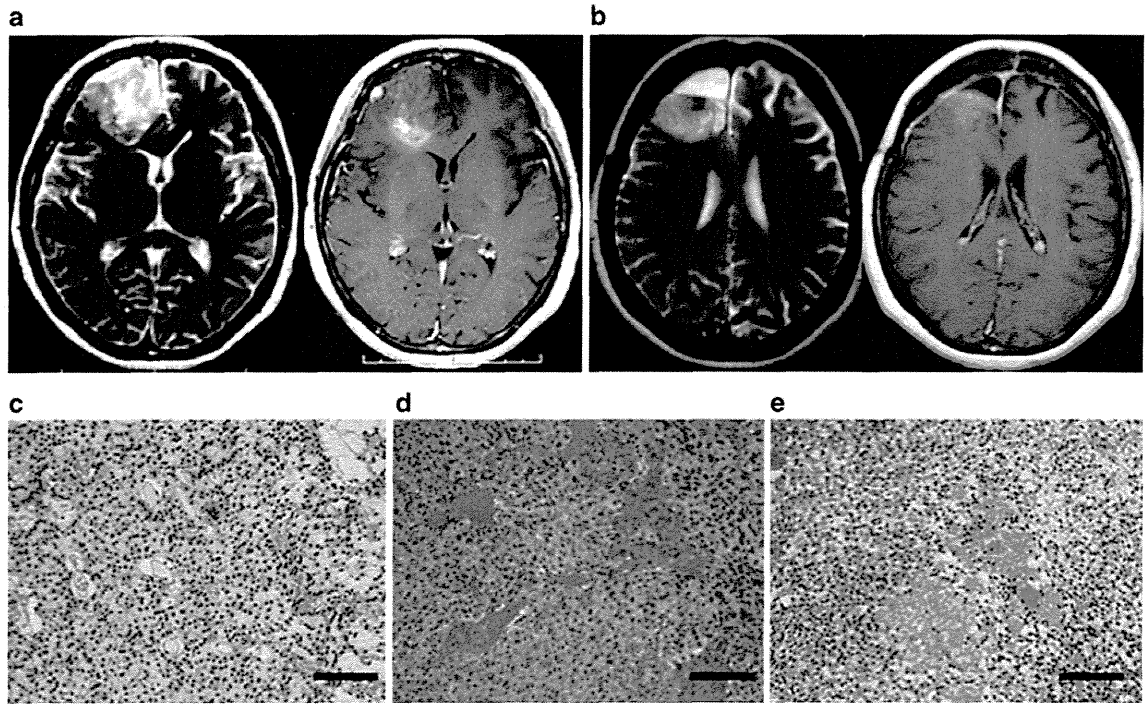

Fig. 2 Representative case with malignant transformation in a 41-year-old woman with right oligodendroglioma in the right frontal lobe. T2-weighted (*left*) and T1-weighted with gadolinium (*right*) magnetic resonance (MR) images at first presentation (**a**), demonstrating that the tumor had a distinct border and slight enhancement. Primary tumor tissues obtained from resection of the tumor consisted of round to oval neoplastic cells with a perinuclear halo but without microvascular proliferation or necrosis, and the diagnosis was oligodendroglioma (**c**). Analysis for IDH1 mutation revealed the tumor had the IDH1 R132H mutation. She did not receive any adjuvant treatments. T2-weighted (*left*) and T1-weighted with gadolinium (*right*) MR images obtained 45 months after the first surgery (**b**), demonstrating that local recurrence developed with slight enhancement. She underwent salvage surgery. Histological examination of recurrent tumor tissues obtained from resection of the tumor revealed that nuclear atypia and cellularity had not increased at recurrence, but new microvascular proliferation (**d**) and tumor necrosis (**e**) had developed. The recurrent tumor was diagnosed as anaplastic oligodendroglioma. ×200. *Bar* = 100 μm

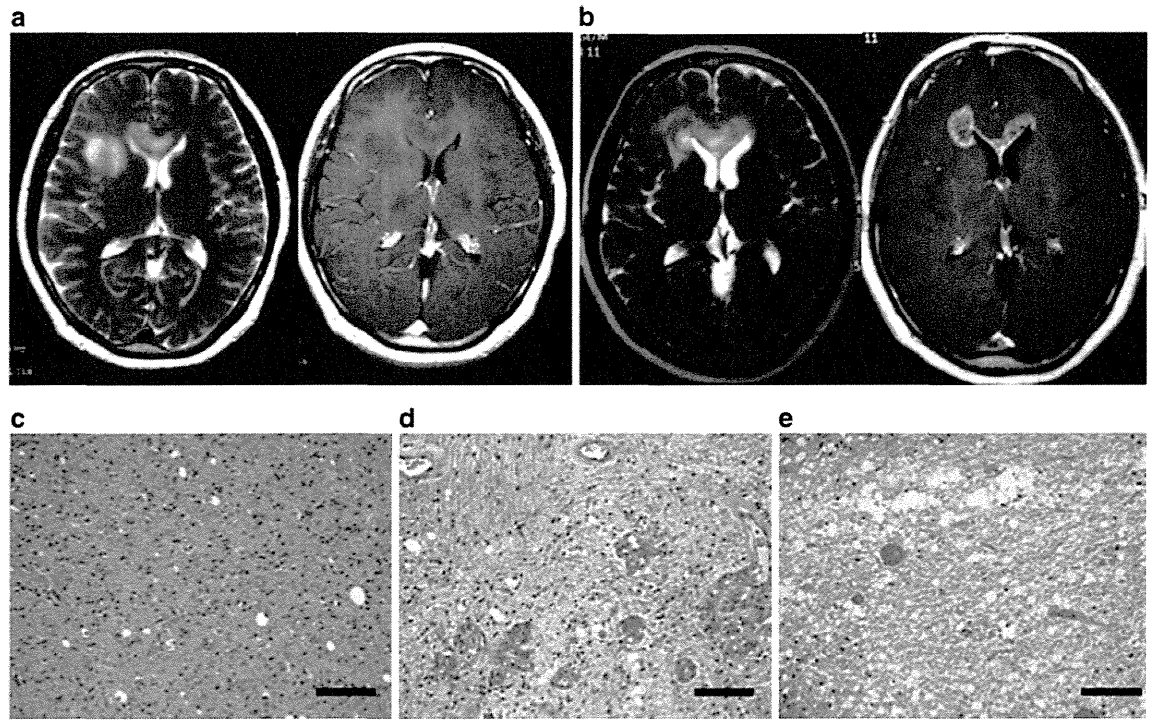

Fig. 3 Representative case with malignant transformation in a 53-year-old woman with oligodendroglioma in the right frontal lobe and corpus callosum. T2-weighted (*left*) and T1-weighted with gadolinium (*right*) magnetic resonance (MR) images at first presentation (**a**), demonstrating that the tumor had an ill-defined tumor border extending to the corpus callosum without enhancement. Primary tumor obtained from open biopsy consisted of round cells with a perinuclear halo but without microvascular proliferation or necrosis, and the diagnosis was oligodendroglioma (**c**). Analysis of IDH1 mutation revealed that the tumor had wild-type IDH1 and IDH2 genes. She received 60 Gy of radiation therapy to the tumor bed. T2-weighted (*left*) and T1-weighted with gadolinium (*right*) MR images obtained 14 months after the first surgery (**b**), demonstrating a strongly enhanced lesion in the right frontal lobe and corpus callosum. Histological examination of recurrent tumor tissues revealed new microvascular proliferations (**d**) without significant changes in cellularity and nuclear atypia. The recurrent tumor was diagnosed as anaplastic oligodendroglioma. Treatment-related coagulation necroses were also observed (**e**). ×200. *Bar* = 100 μm

(Fig. 3). Time to progression was 14, 26, 45, 129, and 236 months, respectively. Newly developed findings of tumor necrosis were present in 4 cases and microvascular proliferation in 5 (Figs. 2, 3). Similar to WHO grade III tumors, it is difficult to diagnose the recurrent tumors after adjuvant therapy as glioblastoma. Our criteria for glioblastoma at recurrence include the existence of astrocytic tumor cells with marked atypia, typical pseudopalisading necrosis. In contrast to the high incidence of malignant transformation in WHO grade II to grade III oligodendroglial tumors, no tumors progressed to glioblastoma or GBMO among the WHO grade III tumors (Fig. 1b). Eight of the 10 WHO grade III tumors had the same histological diagnosis, except for 2 cases with emergence of an astrocytic component (Fig. 1b).

Clinical characteristics of recurrent tumor with or without IDH1 mutation

Analysis for mutation of the IDH1 and IDH2 genes revealed that 13 of the 18 tumors carried mutation in the IDH1 gene. The clinical characteristics are shown in Table 1. The age of onset was younger in the cases with IDH1 mutation ($p = 0.062$). Kaplan–Meier analysis revealed that time to progression was statistically longer in

Table 1 Clinical characteristics of 18 recurrent oligodendroglial tumors with or without IDH1/2 mutation

	IDH1 mutation tumors ($n = 13$)	IDH1/2 wild-type tumors ($n = 5$)	p value
Age at initial presentation (median)	29–70 (41)	52–78 (53)	0.062
Sex (male:female)	9:4	4:1	0.67
Salvage therapy after recurrence			0.99
Radiation therapy or GKS	1	0	
Chemotherapy	9	4	
Both	3	1	
Second recurrence			0.575
Local	5	2	
Dissemination	3	2	

GKS gamma knife radiosurgery

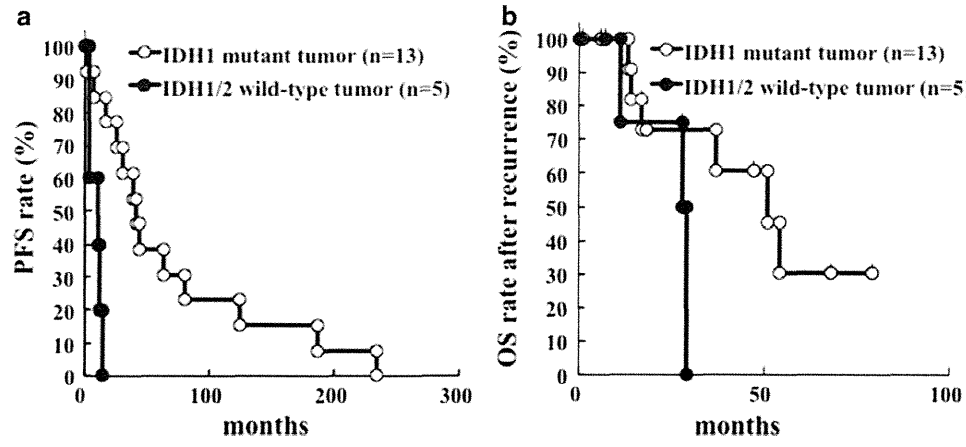

Fig. 4 Kaplan–Meier analysis demonstrating the progression-free survival (PFS) rate after initial surgery (**a**) and the overall survival (OS) rate after first recurrence (**b**) in patients with IDH1-mutation and IDH1/2 wild-type tumors

Table 2 Changes in histological findings for recurrent oligodendroglial tumors with or without IDH1/2 mutation

	IDH1 mutation tumor ($n = 13$)		IDH1/2 wild-type tumor ($n = 5$)	
	Primary	Recurrent	Primary	Recurrent
Histological diagnosis				
OD	3	1	3	2
OA	2	0	0	0
AOD	5	4	1	2
AOA	3	8	1	1
Necrosis				
Tumor necrosis	3	7	0	1
Coagulation necrosis	0	2	0	3
Absent	10	4	5	1
Microvascular proliferation				
Present	6	11	2	2
Absent	7	2	3	3
Ki-67 labeling index (mean) (%)	1.1–42.5 (17.5)[a]	3.3–62.6 (36.3)[a,b]	4.5–13.6 (13.4)	1.3–34.8 (9.2)[b]

OD oligodendroglioma, *OA* oligoastrocytoma, *AOD* anaplastic oligodendroglioma, *AOA* anaplastic oligoastrocytoma

[a,b] $p < 0.05$

IDH1-mutation tumors than in wild-type tumors (median 41 vs. 14 months, $p < 0.005$) (Fig. 4a). After recurrence, all patients received salvage surgery and salvage chemotherapy and/or radiation therapy (Table 1). The patterns of second failure were similar for the IDH1-mutation and IDH1/2 wild-type tumors (Table 1). However, the IDH1-mutation tumor still had the tendency for better prognosis (median 51 vs. 28 months, $p = 0.16$) (Fig. 4b). Six of 13 patients with IDH1-mutation tumor survived for more than 3 years after recurrence, as compared to none with IDH1/2 wild-type tumor (Fig. 4b).

To investigate the better prognosis for recurrent tumors with IDH1 mutation, the histological characteristics and immunohistochemistry for Ki-67 were examined. Contrary to expectations, malignant transformation occurred in 4 of 5 WHO grade II tumors with IDH1 mutations, and in 1 of 3 WHO grade II tumors with wild-type IDH1/2 (Table 2). Newly developed microvascular proliferation and/or tumor necrosis were found in 5 recurrent tumors with IDH1 mutation (Fig. 2; Table 2). Coagulation necrosis, caused by radiation therapy and/or chemotherapy, was predominantly found in 3 of 5 recurrent tumors with wild-type IDH1/2 (Fig. 3; Table 2). Immunohistochemical analysis showed that the Ki-67 labeling index was significantly higher in recurrent tumors with IDH1 mutation than IDH1-mutated primary tumor ($p = 0.012$) and IDH1/2 wild-type recurrent tumors ($p = 0.016$) (Table 2).

Clinical characteristics of recurrent tumor with or without 1p/19q co-deletion

Alternatively, we analyzed the correlations between 1p/19q co-deletions and prognosis in all of the tumors examined and in tumors with IDH1 mutation. Kaplan–Meier analysis revealed that time to progression was longer in 1p/19q co-deleted tumors than in 1p/19q retained tumors (median 63 vs. 12 months, $p < 0.05$, all tumor; median 63 vs. 30 months, $p = 0.077$, tumor with IDH1 mutation). However, when the prognostic value of 1p/19q co-deletions was analyzed in relation to overall survival after recurrence, there was no significant difference between 1p/19q co-deleted and 1p/19q retained tumors (median 51 vs. 28 months, $p = 0.43$, all tumor; median 51 months vs. not reached, $p = 0.90$, tumor with IDH1 mutation). In contrast to the mutation status of IDH1, the rate of malignant transformation and changes in Ki-67 labeling index were not different between 1p/19q co-deleted and 1p/19q retained tumors in all tumors and in tumors with IDH1 mutation.

Changes in nuclear expression of p53 and 1p/19q co-deletions in IDH1-mutation and IDH1/2 wild-type tumors

To explore the genetic changes leading to tumor progression, nuclear expression of p53 and 1p/19q co-deletion was examined in primary and recurrent oligodendroglial tumors. Nuclear expression of p53 and 1p/19q co-deletion were found only in primary tumors with IDH1 mutation in a mutually exclusive fashion, whereas tumors without IDH1 mutation did not have either of them (Fig. 5). Changes of negative to positive nuclear expression of p53 in recurrent tumors occurred in 2 of 6 IDH1-mutation tumors with 1p/19q co-deletions and without nuclear expression of p53 in the primary tumors (Figs. 5, 6, 7). One case had a newly developed astrocytic component at recurrence (Fig. 6), and the other had predominant growth of the oligodendroglial component (Fig. 7). 1p/19q co-deletion was found in 6 of the 18 primary tumors. All cases had the same profile for 1p/19q status (Figs. 5, 6, 7).

Discussion

We reported previously that a significant number of patients with oligodendroglial tumors developed disseminated recurrent disease [13]. Salvage debulking surgery could be performed in 18 of the 36 patients with recurrent oligodendroglial tumors, whereas 14 patients developed disseminated disease at first recurrence. In this study, we focused on the cases of resectable local recurrent disease and reviewed the changes in the histological and genetic findings for recurrent oligodendroglial tumors.

Malignant transformation occurred in 63 % of WHO grade II tumors. Similar incidences of malignant transformation have been reported in WHO grade II tumors [2]. The prospective European Organisation for Research and Treatment of Cancer 22845 study compared the efficacy and safety of postoperative early radiation therapy against WHO grade II tumors to those of postoperative policies of "wait and see" [14]. In that cohort, malignant transformation occurred in 66 % of the wait and see group and in 72 % of the early irradiated group (no significant difference between the groups), and no apparent associations were found between early radiation therapy and malignant transformation. Similarly, 3 of the 5 of our patients with malignant transformation at recurrence did not receive radiation therapy at initial treatment.

Malignant transformation to glioblastoma has been controversial. In contrast to our findings, 18.1 % of AOA and 22.5 % of OA, but none of AOD or OD, were reported to transform to glioblastoma at recurrence [2]. Such differences could be attributed to the diagnostic criteria of AOA and glioblastoma. A new entity of GBMO has been proposed [12, 15, 16], defined as glioblastoma with foci that resemble OD [12]. Based on observations suggesting that the presence of necrosis is associated with worse prognosis in AOA [17], AOA with necrosis was classified as GBMO in the WHO classification [12]. GBMO has better prognosis than "classic" glioblastoma and worse prognosis than AOD, anaplastic astrocytoma, and AOA without necrosis [17]. Although AOA with necrosis could be an entity independent of other tumors, no definite criteria have been established to differentiate GBMO, AOA with or without necrosis, and glioblastoma [18] in primary tumors. Furthermore, the differential diagnosis of this

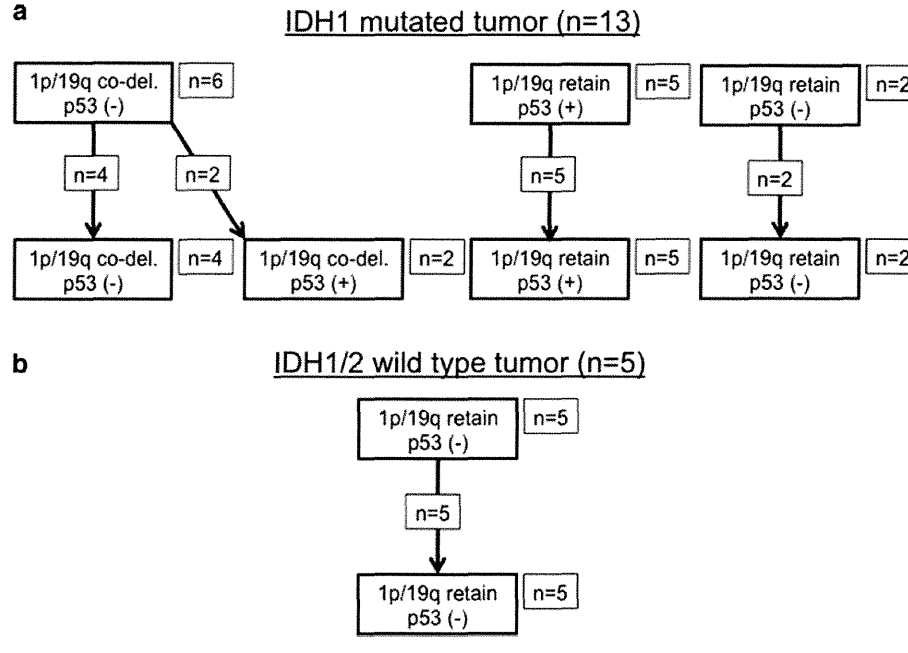

Fig. 5 Changes in the genetic mutations of primary and recurrent oligodendroglial tumors with (**a**) or without (**b**) IDH1 mutation. *1p/19 co-del.* loss of heterozygosity of chromosomes 1p and 19q, *1p/19q retain* retention of heterozygosity of chromosomes 1p and 19q, *p53* (+) positive for nuclear expression of p53, *p53* (−) negative for nuclear expression of p53

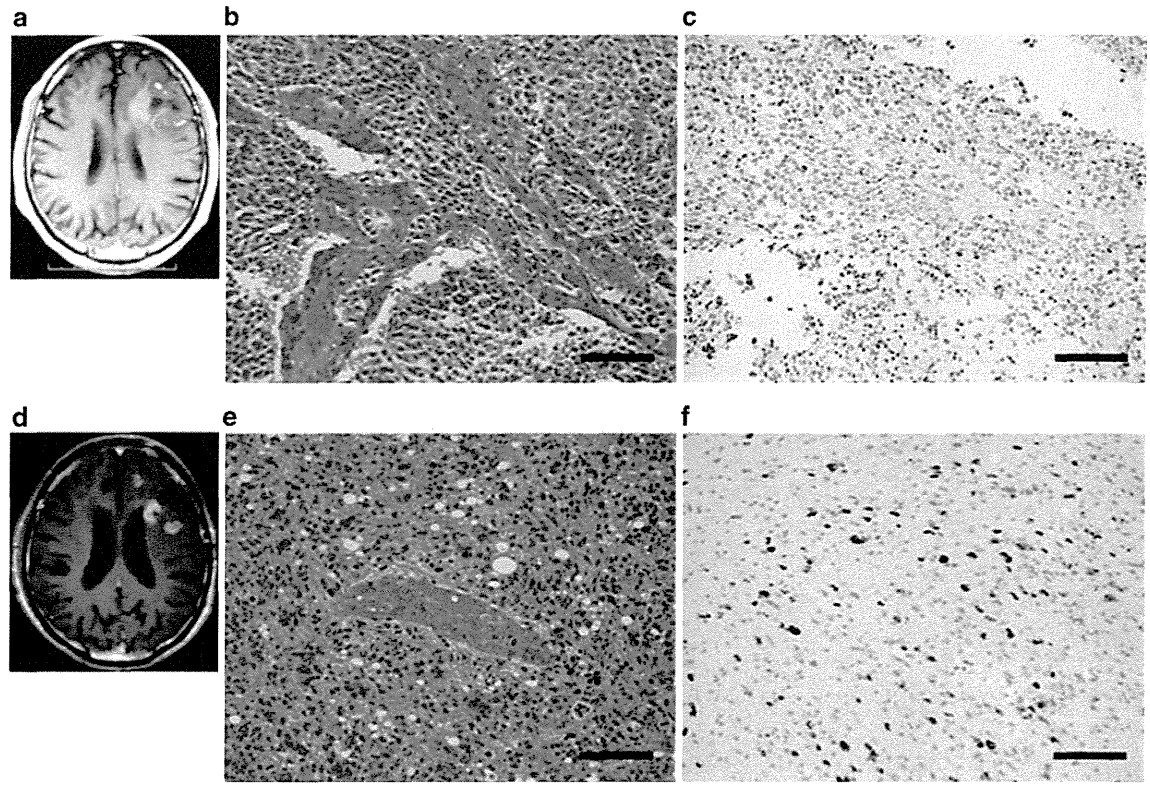

Fig. 6 Representative case of nuclear expression of p53 changing from negative to positive at recurrence in a 70-year-old man with anaplastic oligodendroglioma in the left frontal lobe. T1-weighted magnetic resonance (MR) image with gadolinium at first presentation (**a**), demonstrating heterogeneous enhancement of the tumor. Primary tumor tissues obtained from resection of the tumor consisted of round to oval neoplastic cells with a perinuclear halo, significant nuclear atypia, and increased cellularity. Microvascular proliferations were also found (**b**). Immunohistochemistry for p53 revealed that tumor cells were negative for p53 (**c**). Analysis for IDH1 mutation and fluorescent in situ hybridization for chromosomes 1p and 19q revealed that the tumor had both IDH1 mutation and 1p/19q co-deletion. The diagnosis was anaplastic oligodendroglioma. He received 72 Gy of hyperfractionated radiation therapy to the tumor bed. T1-weighted MR image with gadolinium obtained 45 months after the first surgery (**d**), demonstrating that local recurrence developed with slight enhancement. He underwent salvage surgery. Emergence of an astrocytic component, as well as higher cellularity and the development of tumor necrosis, was found (**e**). Immunohistochemistry revealed that nuclear expression of p53 had changed from negative to positive at recurrence (**f**), whereas the recurrent tumor had 1p/19q co-deletion. The diagnosis was anaplastic oligoastrocytoma. ×200. *Bar* = 100 μm

entity was more confusing in recurrent tumors because prior treatment could cause coagulation necrosis due to ischemia through chemotherapy and radiation therapy associated vascular damage. We agree that it is sometimes difficult to distinguish the ischemic coagulation necrosis associated with vascular damage from the so-called "tumor necrosis" that occurs spontaneously due to the relative hypoxia caused by high proliferative potential. In this study, we considered "tumor necrosis" to consist of "dirty-looking" necrobiotic neoplastic cells surrounded by the tumor cells with high viability, and "coagulation necrosis" to consist of homogeneously necrotic ghost cells that do not appear to be surrounded by viable tumor cells. Based on this classification, 5 cases had recurrent disease of AOA with newly developed tumor necrosis. Two of them did not receive any adjuvant therapy, and the remaining 3 underwent radiochemotherapy. The primary tumors were OD in 1, OA in 2, AOD in 1, and AOA without necrosis in 1. Whether AOA with newly developed tumor necrosis should be regarded as a malignant transformation or not is an important consideration when assessing the effects of prior treatments and scheduling salvage treatments in such cases. On the contrary, we found coagulation necrosis in 5 recurrent tumors, and all of them received radiation therapy before recurrence. Initial diagnosis was OD in 2 and AOD in 3. One case with OD developed glomeruloid microvascular proliferation with coagulation necrosis at recurrence, and was diagnosed as a malignant transformation from WHO grade II to III tumor—not to glioblastoma, because we did not find pseudopalisading or tumor necrosis, or an astrocytic component. Similarly, the remaining 4 cases did not have these features either, so these cases received the same histological diagnosis as the primary tumors: not glioblastoma or GBMO.

Oligodendroglial tumors carrying IDH1 or IDH2 mutations have longer progression-free survival and overall

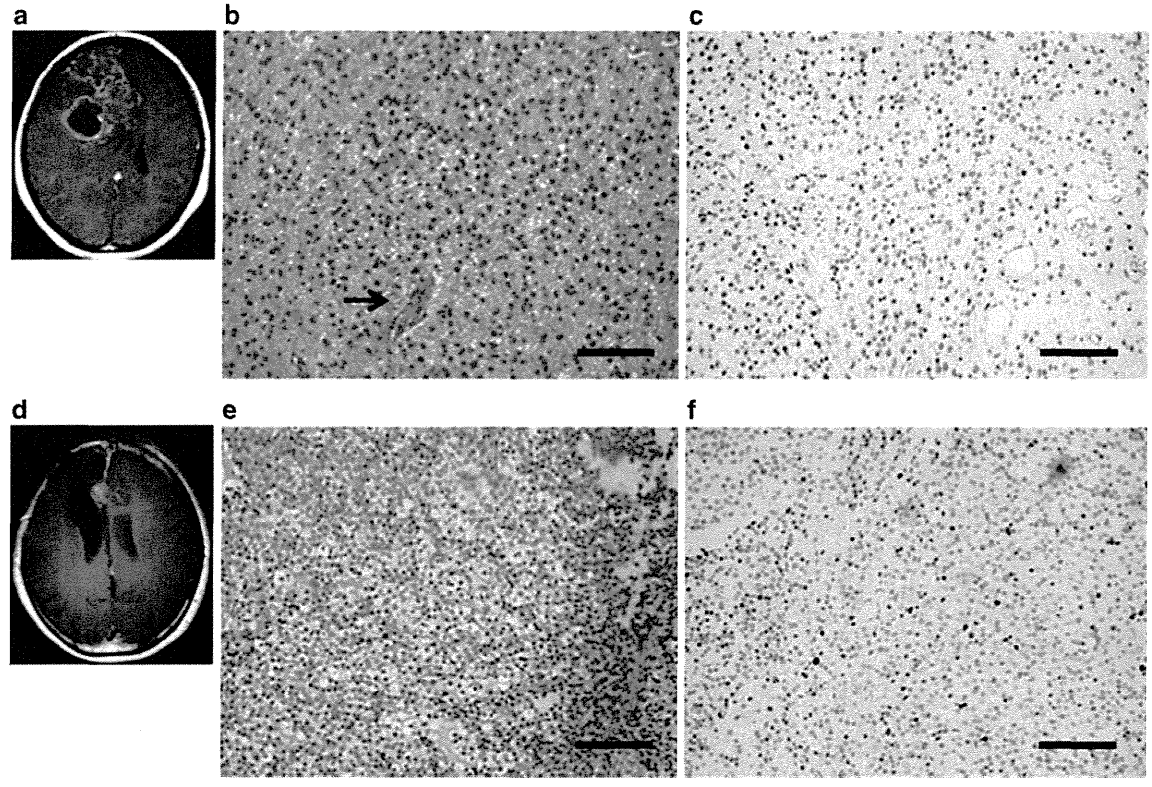

Fig. 7 Representative case of nuclear expression of p53 changing from negative to positive at recurrence in a 40-year-old woman with anaplastic oligoastrocytoma in the right frontal lobe. T1-weighted magnetic resonance (MR) image with gadolinium at first presentation (**a**), demonstrating heterogeneous enhancement of the tumor with cyst formation. Primary tumor tissues obtained from tumor resection consisted of round cells with a perinuclear halo and gemistocytic neoplastic astrocytes. Microvascular proliferation was also found (**b** *arrow*). Immunohistochemistry for p53 revealed that the tumor cells were negative for p53 (**c**). Analysis for IDH1 mutation and fluorescent in situ hybridization for chromosomes 1p and 19q revealed that the tumor had both IDH1 mutation and 1p/19q co-deletion. The diagnosis was anaplastic oligoastrocytoma. She received 72 Gy of hyperfractionated radiation therapy to the tumor bed and administration of nimustine hydrochloride. T1-weighted MR image with gadolinium obtained 95 months after the first surgery (**d**), demonstrating that local recurrence had developed with enhancement. Increase in the oligodendroglial component was found (**e**). Immunohistochemistry revealed that nuclear expression of p53 changed from negative to positive at recurrence (**f**), whereas the recurrent tumor had 1p/19q co-deletion. The diagnosis was anaplastic oligoastrocytoma. ×200. *Bar* = 100 μm

survival rates [8–10]. We found recurrent tumors with IDH1 mutation to have a long latency to progression, a higher rate of malignant transformation, and elevated proliferation activities. Despite such histological features, recurrent tumors with IDH1 mutation tended to have better outcome. In contrast, IDH1/2 wild-type tumors frequently showed mixtures of coagulation necrosis and degenerated tumor or normal cell tumor, and low proliferation activities, possibly because IDH1/2 wild-type recurrent tumors progressed early after initial treatment, before the effect disappeared. Considering the absence of apparent differences in salvage therapies and patterns of failure, tumors with IDH1 mutation could remain less aggressive or more sensitive to treatment, even at recurrence.

We explored the changes in the representative genetic aberrations, including nuclear expression of p53 and 1p/19q co-deletions, to clarify the molecular mechanisms leading to tumor progression in IDH1-mutation or IDH1/2 wild-type tumors. Previously, changes in chromosomal aberrations have been reported [3, 4]. Tumor with 1p/19q co-deletion demonstrated the same aberrations in recurrent tumor, whereas recurrent tumor frequently showed increased polysomies, rather than any specific chromosomal changes, and deletions of p16 loci [3]. In our series, no changes in 1p/19q status were found at recurrence. However, nuclear expression of p53 changed from negative to positive in 2 IDH1-mutation tumors. WHO grade II gliomas carrying IDH mutation had either 1p/19q or aberrant nuclear expression of p53, and these aberrations were mutually exclusive. We found that 11 of 13 primary tumors with IDH1 mutation carried one of these aberrations exclusively. Interestingly, 2 tumors with both IDH1 mutation and 1p/19q co-deletion also showed aberration of nuclear expression of p53 at recurrence. This finding suggests that de novo p53 mutation or the proliferation of a small subset of cells with nuclear expression of p53 could lead to tumor progression in some IDH1-mutation oligodendroglial tumors. The biphasic type of AOA consists of

distinct areas with 1p/19q co-deletion and nuclear expression of p53 [19]. We found that a small subset of tumors contain cells with nuclear expression of p53, as shown in Figs. 5 and 6. Therefore, we presume that small numbers of the cells with aberrant function of p53 proliferated in the process of IDH1-mutation tumor recurrence.

In conclusion, this study found that a high rate of malignant transformation occurred in WHO grade II oligodendroglial tumors at recurrence, which may involve p53 in tumors with IDH1 mutation and 1p/19q co-deletion. Recurrent tumors with IDH1 mutation had a more aggressive histological phenotype despite their better prognosis.

References

1. Committee of Brain Tumor Registry of Japan (2009) Report of Brain Tumor Registry of Japan (1984–2000), 12th edition. Neurol Med Chir (Tokyo) 49 Suppl:i–vii, 1–101
2. Jaeckle KA, Decker PA, Ballman KV et al (2011) Transformation of low grade glioma and correlation with outcome: an NCCTG database analysis. J Neurooncol 104:253–259
3. Fallon KB, Palmer CA, Roth KA et al (2004) Prognostic value of 1p, 19q, 9p, 10q, and EGFR-FISH analyses in recurrent oligodendrogliomas. J Neuropathol Exp Neurol 63:314–322
4. Campbell BA, Horsman DE, Maguire J et al (2008) Chromosomal alterations in oligodendroglial tumours over multiple surgeries: is tumour progression associated with change in 1p/19q status? J Neurooncol 89:37–45
5. Balss J, Meyer J, Mueller W, Korshunov A, Hartmann C, von Deimling A (2008) Analysis of the IDH1 codon 132 mutation in brain tumors. Acta Neuropathol 116:597–602
6. Parsons DW, Jones S, Zhang X et al (2008) An integrated genomic analysis of human glioblastoma multiforme. Science 321:1807–1812
7. Sonoda Y, Kumabe T, Nakamura T et al (2009) Analysis of IDH1 and IDH2 mutations in Japanese glioma patients. Cancer Sci 100:1996–1998
8. Metellus P, Coulibaly B, Colin C et al (2010) Absence of IDH mutation identifies a novel radiologic and molecular subtype of WHO grade II gliomas with dismal prognosis. Acta Neuropathol 120:719–729
9. Li S, Yan C, Huang L, Qiu X, Wang Z, Jiang T (2012) Molecular prognostic factors of anaplastic oligodendroglial tumors and its relationship: a single institutional review of 77 patients from China. Neuro Oncol 14:109–116
10. van den Bent MJ, Dubbink HJ, Marie Y et al (2010) IDH1 and IDH2 mutations are prognostic but not predictive for outcome in anaplastic oligodendroglial tumors: a report of the European Organization for Research and Treatment of Cancer Brain Tumor Group. Clin Cancer Res 16:1597–1604
11. Ichimura K, Pearson DM, Kocialkowski S et al (2009) IDH1 mutations are present in the majority of common adult gliomas but rare in primary glioblastomas. Neuro Oncol 11:341–347
12. Louis DN, Ohgaki H, Wiestler OD, Cavenee WK (2007) WHO classification of tumours of the central nervous system. IARC, Lyon
13. Kanamori M, Kumabe T, Sonoda Y, Nishino Y, Watanabe M, Tominaga T (2009) Predictive factors for overall and progression-free survival, and dissemination in oligodendroglial tumors. J Neurooncol 93:219–228
14. van den Bent MJ, Afra D, de Witte O et al (2005) EORTC Radiotherapy and Brain Tumor Groups and the UK Medical Research Council. Long-term efficacy of early versus delayed radiotherapy for low-grade astrocytoma and oligodendroglioma in adults: the EORTC 22845 randomised trial. Lancet 366: 985–990
15. Kraus JA, Lamszus K, Glesmann N et al (2001) Molecular genetic alterations in glioblastomas with oligodendroglial component. Acta Neuropathol 101:311–320
16. He J, Mokhtari K, Sanson M et al (2001) Glioblastomas with an oligodendroglial component: a pathological and molecular study. J Neuropathol Exp Neurol 60:863–871
17. Miller CR, Dunham CP, Scheithauer BW, Perry A (2006) Significance of necrosis in grading of oligodendroglial neoplasms: a clinicopathologic and genetic study of newly diagnosed high-grade gliomas. J Clin Oncol 24:5419–5426
18. Marucci G (2011) The effect of WHO reclassification of necrotic anaplastic oligoastrocytomas on incidence and survival in glioblastoma. J Neurooncol 104:621–622
19. Qu M, Olofsson T, Sigurdardottir S et al (2007) Genetically distinct astrocytic and oligodendroglial components in oligoastrocytomas. Acta Neuropathol 113:129–136
20. Perry A, Brat DJ (2010) Practical surgical neuropathology. Elsevier, Philadelphia, p 421

Clinical Neuropathology, Vol. 31 – No. 2/2012 (67-76)

ISSN 0722-5091

DOI 10.5414/NP300402
e-pub: February 29, 2012

Pathologic diversity of glioneuronal tumor with neuropil-like islands: A histological and immunohistochemical study with a special reference to isocitrate dehydrogenase 1 (IDH1) in 5 cases

Keisuke Ishizawa[1], Takanori Hirose[2], Kazuhiko Sugiyama[3], Teruyoshi Kageji[4], Sumihito Nobusawa[5], Taku Homma[1], Takashi Komori[6] and Atsushi Sasaki[1]

[1]Department of Pathology, Saitama Medical University, Saitama, [2]Department of Diagnostic Pathology, Tokushima Prefectural Central Hospital, Tokushima, [3]Department of Neurosurgery, Hiroshima University, Hiroshima, [4]Department of Neurosurgery, Tokushima University, Tokushima, [5]Department of Human Pathology, Gunma University Graduate School of Medicine, Gunma, and [6]Department of Laboratory Medicine and Pathology (Neuropathology), Tokyo Metropolitan Neurological Hospital, Tokyo, Japan

Key words
glioneuronal tumor with neuropil-like islands – isocitrate dehydrogenase 1 (IDH1) – synaptophysin – immunohistochemistry – mutation analysis

Abstract. Glioneuronal tumor with neuropil-like islands (GTNI) is featured by "neuropil-like islands (NIs)" within dominating astroglial components. Isocitrate dehydrogenase (IDH) mutations, particularly IDH1 R132H (G395A), are found in WHO Grade II and III diffuse gliomas as well as secondary, but not primary, glioblastomas. We reviewed 5 cases of GTNI, and assessed histology and immunohistochemistry with various antibodies, including those for IDH1 R132H, as well as direct DNA sequencing for *IDH1 G395A*. NIs were variable in morphology, and constantly synaptophysin-positive and glial fibrillary acidic protein-negative. The glioma components were primary glioblastoma in 2 cases, anaplastic astrocytoma in 1 and anaplastic oligoastrocytoma in 2. The IDH1 R132H was expressed in the 2 cases with oligoastrocytoma: In 1, NIs and the astrocytoma-like area as well as the oligodendroglioma-like area were positive. In the other, only the oligodendroglioma-like area was positive. The mutation analysis performed on the latter case with DNA separately sampled from the oligodendroglioma-like area and the astrocytoma-like area detected *IDH1 G395A* in both areas. We have shown diverse pathologic aspects of GTNI. Also, we have shown that the expression of IDH1 R132H in GTNI is largely concordant with that in diffuse gliomas, and that it can be dependent on each histologic component although the mutant *IDH1* gene is ubiquitously present within the tumor.

Received
May 2, 2011;
accepted in revised form
September 1, 2011

Correspondence to
Keisuke Ishizawa, MD
Department of Pathology, Saitama Medical University, Morohongo 38, Moroyama-town, Irumagun, Saitama, 350-0495, Japan
ishizawa@saitama-med.ac.jp

Introduction

Glioneuronal tumor with neuropil-like islands (GTNI) is a recently advocated entity that is marked by delimited, round to oval islands composed of a delicate, neuropil-like matrix within WHO Grade II or III astrocytoma [1]. The islands, named "neuropil-like islands (NIs)", are populated by small, round, and oligodendrocyte-like cells, plus larger, hyperchromatic cells or mature-appearing neurons [1]. Although GTNI has been placed under the spectrum of astrocytoma in the latest WHO classification of brain tumors [2], the exact position of the tumor in the nosology of brain tumors remains elusive and unsolved.

A recent research in oncology has found a series of isocitrate dehydrogenase (IDH) mutations, particularly IDH1 R132H (G395A) mutation, to be a cardinal genetic alteration of gliomas [3]. Now IDH1 and IDH2 mutations are placed most upstream in the cascade of genetic events of WHO Grade II and III astrocytomas, oligodendrogliomas, oligoastrocytomas, and WHO Grade IV secondary glioblastomas [4, 5]. On the other hand, the issue of IDH in GTNI has just been tackled in only a few investigations [6, 7].

Recently we have encountered a new series of GTNI that is composed of 5 cases. In this report, we attempted to provide further

Table 2. Pathologic findings of neuropil-like islands

Case	Morphology	Syn	NFP	NeuN	NSE	GFAP	Olig2	p53	Ki-67
1	Round, ganglioid cells	++	++	+/–	++	–	–	+	+/–
2	Round	++	–	ND	ND	–	+	+	+/–
3	Irregular, pleomorphism	++	++	+/–	++	–	++	+/–	+/–
4	Irregular, cell clusters	++	–	–	++	–	+/–	–	–
5	Round	++	–	–	++	–	++	+/–	++

Syn = synaptophysin; NFP = neurofilament protein; NSE = neuron-specific enolase; GFAP = glial fibrillary acidic protein; ND = no data.

Table 3. Pathologic findings of glioma components

Case	Glial morphology	Area	Syn	NFP	NeuN	NSE	GFAP	Olig2	p53	Ki-67
1	Glioblastoma*	Ast	–	–	+/–	++	++	+/–	++	+
2	Anaplastic astrocytoma	Ast	–	–	ND	ND	++	+	+	+
3	Anaplastic oligoastrocytoma	Ast	–	–	–	++	++	++	+/–	+
		Oligo	+/–	–	–	++	+	++	ND	++
4	Anaplastic oligoastrocytoma	Ast	–	–	–	++	++	+/–	+/–	+/–
		Oligo	+/–	–	–	++	+	++	+/–	+
5	Glioblastoma*	Ast	–	–	–	++	++	+	++	+

Ast = astrocytoma-like area; Oligo = oligodendroglioma-like area; Syn = synaptophysin; NFP = neurofilament protein; NSE = neuron-specific enolase; GFAP = glial fibrillary acidic protein; ND = no data; * = primary glioblastoma.

(Case 2, Figure 2D; Case 4, Figure 2H; Case 5, Figure 2J), but there were dysmorphic ones, such as those containing multiple nuclei (Case 3, Figure 2F). In 1 case (Case 1) a few larger ganglioid cells were noted (Figure 2B). The number of NIs was regionally heterogeneous, but a maximum of up to 10 NIs was observed with the magnification of × 400. The "rosette" arrangement of cells, which was previously emphasized [1], was a minor finding in the present cases. Mitosis was not found in NIs.

The glioma components were variable as well (Table 3). They were glioblastoma in 2 cases (Case 1, Figure 3A; Case 5, Figure 3C) and anaplastic astrocytoma in 1 (Case 2, Figure 3B). In the 2 cases with glioblastoma, there was no previous history of the tumor; thus the tumors were considered to be primary glioblastomas. In Case 3, the glioma component contained two elements. One was an astrocytoma-like area featuring atypical astrocytic cells (Figure 3D). The other contained atypical cells having hyperchromatic nuclei (Figures 3E, F). Albeit some variation in size and shape, the nuclei tended to be round and have peri-nuclear haloes. These cells were partially arranged in a palisade. Homer Wright rosettes were not identified. Minigemistocytes were scattered. Although microvascular proliferation and necrosis were absent, mitoses were occasionally found. These histologic features were most consistent with anaplastic oligodendroglioma. Taken together, the glioma component of Case 3 was diagnosed as an anaplastic oligoastrocytoma. The glioma component of Case 4 had two elements as well: one showed atypical astrocytic cells (Figure 3G) and the other showed atypical cells having round nuclei and peri-nuclear haloes in addition to microvascular proliferation and mitoses (Figure 3I). These two elements abutted against each other with a clear border (Figure 3H). Taken together, the glioma component of Case 4 was also diagnosed as an anaplastic oligoastrocytoma. In both Case 3 and Case 4, NIs were present in the astrocytoma-like areas, but not in the oligodendroglioma-like areas.

Immunohistochemical results

NIs

In all cases NIs were positive (++) for Syn and negative (–) for GFAP. Not only

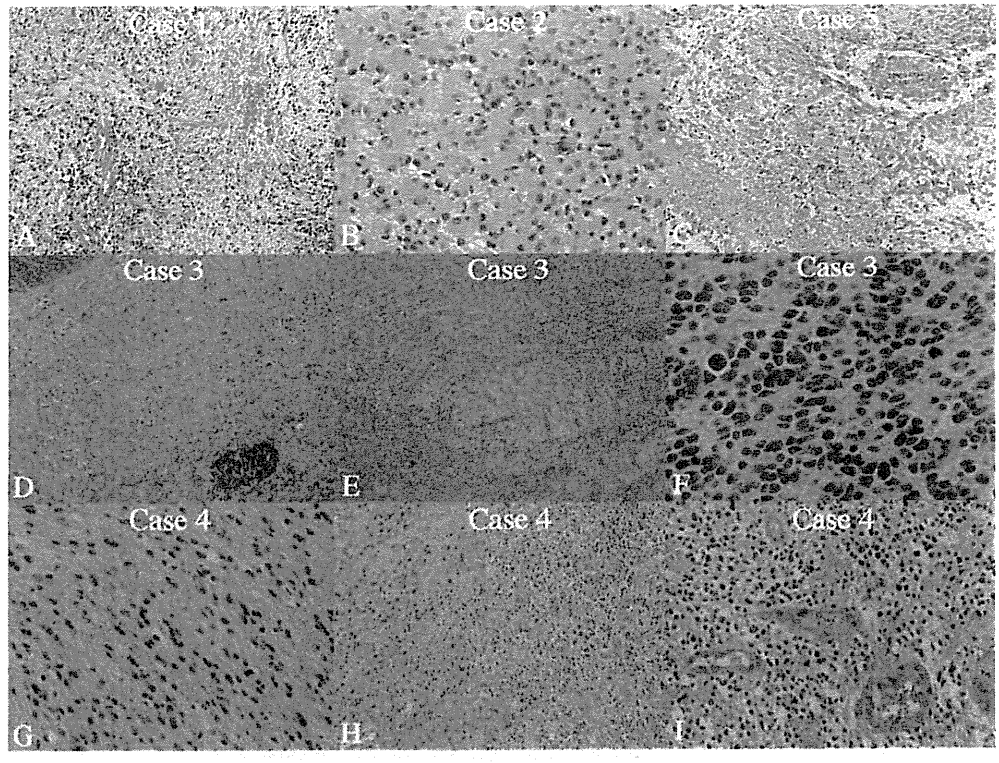

Figure 3. The histological results of glioma components of the 5 tumors. (H&E stain). A: Case 1. Proliferation of anaplastic astrocytes, microvascular proliferation, and necroses characterize this tumor (× 200). B: Case 2. Proliferation of gemistocytic astrocytes characterizes this tumor (× 200). C: Case 5. Proliferation of anaplastic astrocytes, microvascular proliferation, and necroses characterize this tumor (× 200). D, E, F: Case 3. In this tumor, in addition to an astrocytoma-like area (D), a hypercellular area, which is composed of hyperchromatic cells having peri-nuclear haloes (F), abuts against the astrocytoma-like area (E) (D, × 100; E, × 40; F, × 400). G, H, I: Case 4. As in Case 3, this tumor contains an astrocytoma-like area (G) and a hypercellular area (I), and the two areas abut against each other (H). The cells in the latter are round and have peri-nuclear haloes (I). Note microvascular proliferation in the latter (I) (G, × 200; H, × 100; I, × 200).

in the 3 cases with spherical NIs (Figures 4A, B), but also in the 2 cases with irregular NIs (Case 3, Figures 4C, D; Case 4, Figures 4E, F), this immunophenotype for Syn and GFAP was strictly retained. Syn was mostly detected in the matrix, but also in some cells with cytoplasmic immunoreactivity. NSE was detected in all cases available (4/4 cases). NFP (Figures 5A, B) was detected in 2 out of the 5 cases: the anti-NFP antibodies labeled the matrices as well as the cells. The NeuN antibody (Figures 5C, D) labeled the nuclei and soma of cells in 2 out of the 5 cases; these were the same 2 cases that showed the NFP-immunoreactivity (Table 2). The immunoreactivity for Olig2 was detected in 4 out of the 5 cases. p53 was detected in all but Case 4. The Ki-67 labeling index (MIB-1 index) was +/– in 3 cases (Cases 1 – 3, Figure 5E) and was ++ in 1 (Case 5, Figure 5F). Ki-67 was not detected in the NIs of Case 4.

Glioma components

In Cases 1, 2 and 5, which were GTNIs with high-grade astrocytoma, the neuronal markers (Syn and NFP) were negative (–) and the glial marker (GFAP) was positive (++). In Cases 3 and 4, which were GTNIs with oligoastrocytoma, the astocytoma-like areas were positive (++) for GFAP and negative (–) for neuronal markers. Except for weak (+/–) immunoreactivity for Syn, the oligodendroglioma-like areas were negative (–) for neuronal markers. The MIB-1 index tended to be higher for the oligodendroglioma-like areas than it was for the astocytoma-like areas.

Immunohistochemical analysis for IDH1 R132H

Two out of the 5 cases showed unequivocal immunoreactivity for IDH1. The positive

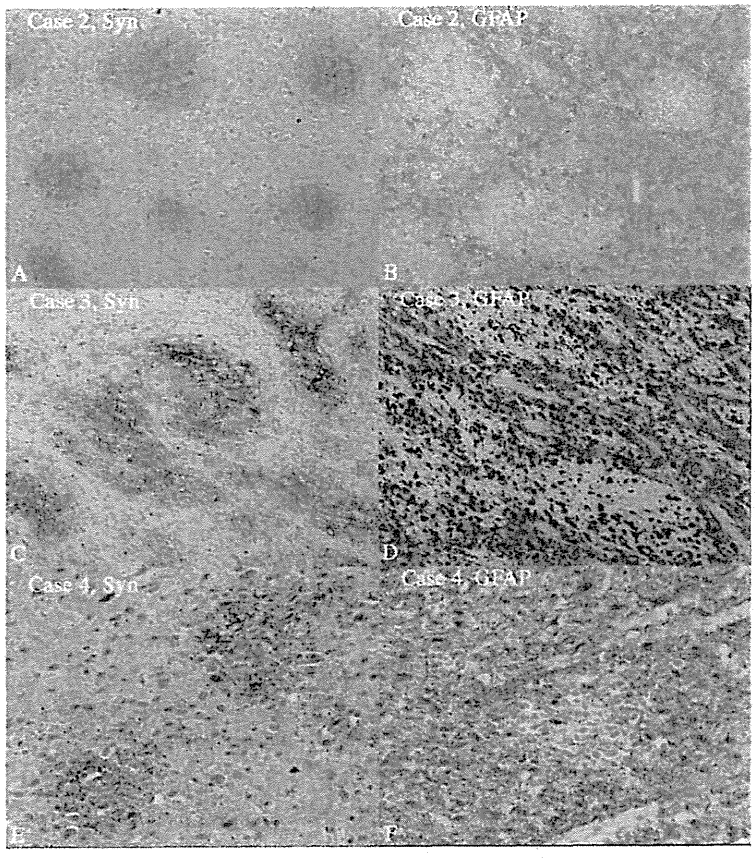

Figure 4.

Figure 4. The immunohistochemical results of neuropil-like islands (NIs) for synaptophysin (Syn) and glial fibrillary acidic protein (GFAP) in the tumors. A, B: In Case 2, the NIs are spherical; and they are positive for Syn in the matrix (A), but not for GFAP (B) (A, B; × 100). C, D: In Case 3, the NIs are irregular; but even in this case, they are positive for Syn (C), but not for GFAP (D) (C, D; × 100). E, F: In Case 4, the NIs are scant of neuropil-like matrix; but even in this case, they are positive for Syn (E), but not for GFAP (F) (E, F; × 200).

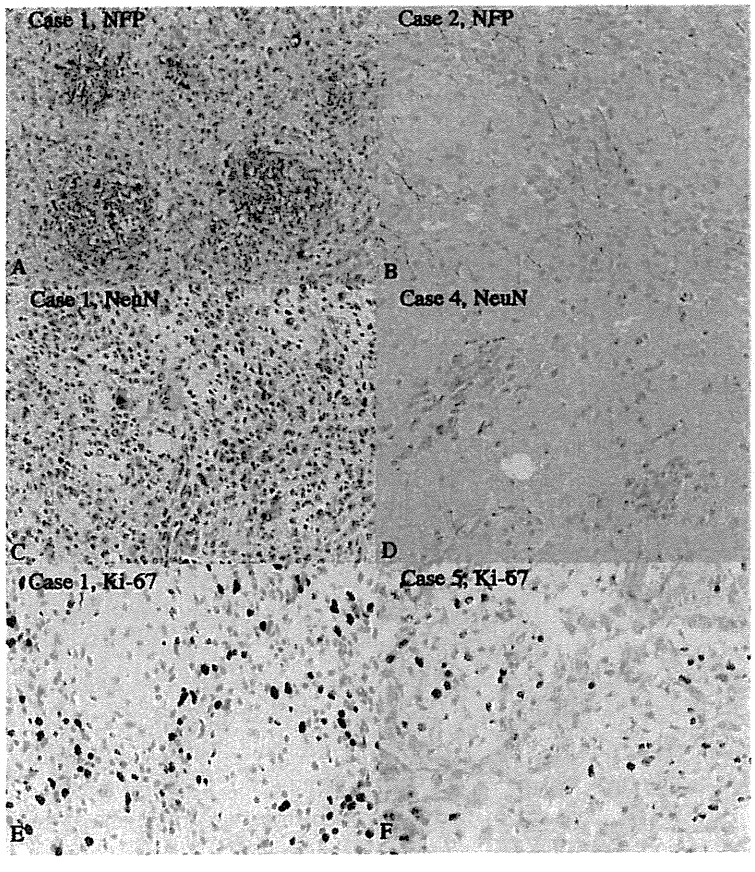

Figure 5.

Figure 5. The immunohistochemical results of neuropil-like islands (NIs) for neurofilament protein (NFP), NeuN and Ki-67 in the tumors. A, B: In Case 1, the NIs are strongly positive for NFP in the matrix as well as in the soma of cells (A), while in Case 2, the NIs are negative for NFP (B) (NFP immunostain: A, B; × 200). C, D: In Case 1, there are some cells that are positive for NeuN in the nucleus and the cytoplasm (C), while in Case 4, the NIs are negative for NeuN (D) (NeuN immunostain: C, D; × 200). E, F: Generally speaking, the cells in the NIs show a low proliferative activity: Note that the NIs in Case 1 are scant of Ki-67-positive nuclei (E). But in 1 case (Case 5) they show a high profilerative activity: Note that the NIs in Case 5 contain many Ki-67-positive nuclei (F) (Ki-67 immunostain: E, F; × 400)

cases were Cases 3 and 4, that is, the GTNIs with anaplastic oligoastrocytoma. In Case 3, both the Syn-positive area and the GFAP-positive area were positive for IDH1. But interestingly, the IDH1-positive area (Figure 6A) corresponded to the Syn-positive area (Figure 6B) rather than the GFAP-positive area (Figure 6C) in some fields. The neuropil-like matrices and the cells inhabiting NIs were stained with the anti-IDH1 antibody. Another component, the oligodendroglioma-like area, was intensely positive for IDH1 (Figure 6D). In Case 4, neither the Syn-positive area (Figure 6F) nor the GFAP-positive area (Figure 6G) was positive for IDH1 (Figure 6E); however, as in Case 3, the oligodendroglioma-like area was intensely positive for IDH1 (Figure 6H).

IDH1 mutation analysis

In Case 4, the mutant *IDH1 G395A* was detected in both the oligodendroglioma-like area and the astrocytoma-like area (Figure 7).

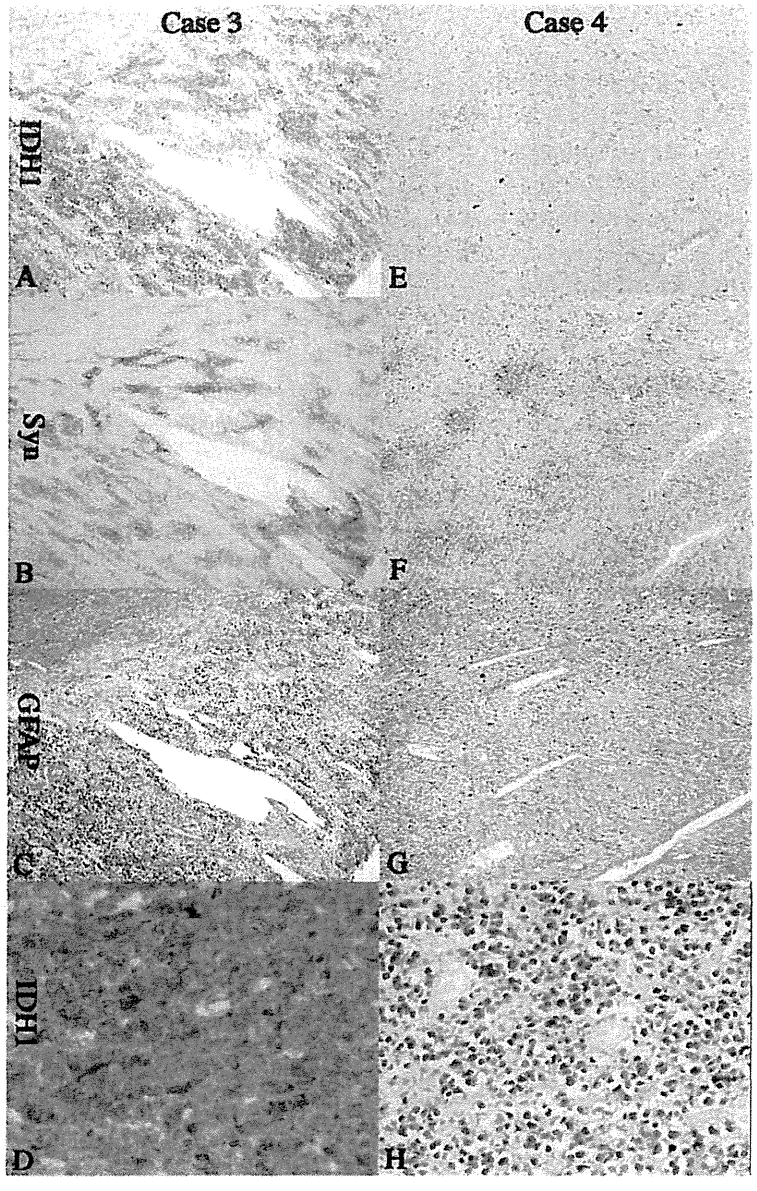

Figure 6. The immunohistochemical results for IDH1 R132H in Cases 3 and 4. Serially immunostained sections (A – D and E – H) are shown. A – D: Case 3. The IDH1-positive areas (A) correspond to Syn-positive areas (B) rather than GFAP-positive areas (C). The oligodendroglioma-like area shows intense immunoreactivity for IDH1 (D) (A – C, × 40; D, × 400). E – H: Case 4. In this case, neither Syn-positive areas (F) nor GFAP-positive areas (G) show immunoreactivity for IDH1 (E). As in Case 3, the oligodendroglioma-like area shows intense immunoreactivity for IDH1 (H) (E – G, × 100; H, × 400). Syn = synaptophysin; GFAP = glial fibrillary acidic protein.

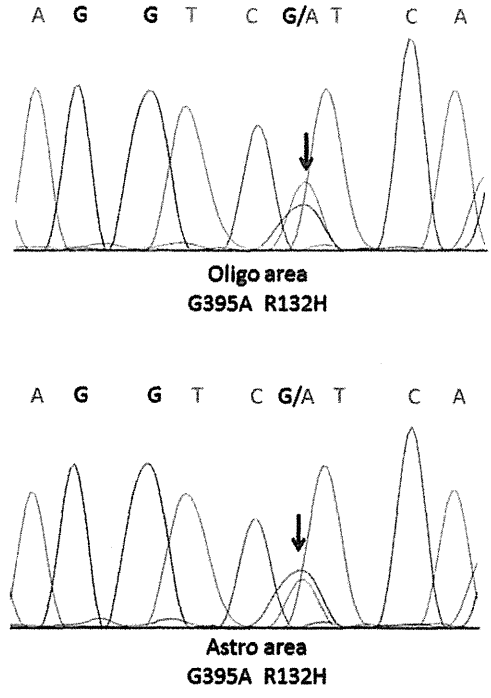

Figure 7. The result of the *IDH1* mutation analysis on Case 4 is shown. In this case, the substitution of guanine by adenine at position 395 (G395A) was detected in both the oligodendroglioma-like area and the astrocytoma-like area. Oligo area = oligodendroglioma-like area; Astro area = astrocytoma-like area.

Discussion

In the original paper on GTNI [1] or some case reports on GTNI [9, 10], GTNIs were associated with WHO Grade II or III astrocytomas. In line with these reports, GTNI was defined as a tumor with WHO Grade II or III astrocytoma in the latest WHO classification of brain tumors [2]. However, a careful look at the medical literature shows that the gliomas associated with GTNI are not limited to WHO Grade II or III astrocytomas, but encompass a wide variety of gliomas. The case by Vajtai et al. [11] was a GTNI with a glioblastoma. The series by Barbashina et al. [12], which included 8 cases of GTNI, contained a case with a high-grade glioma characterized by a high MIB-1 index (20%), microvascular proliferation, and necrosis. As for the present series of GTNI, the glioma components of the 5 cases were glioblastoma (primary glioblastoma) in 2 cases (Cases 1 and 5), anaplastic astrocytoma in 1 (Case 2), and anaplastic oligoastrocytoma in 2 (Cases 3 and 4). The diagnoses of Cases 1, 2 and 5 could be unanimous since these cases showed typical NIs, i.e., delimited areas containing neuropil-like matrices and small, round cells as well as a few ganglioid cells [1] against the background of astrocytoma. On the other hand, Cases 3 and 4 are likely to pose a diagnostic challenge since the NIs of Case 3 were like pale, irregular streaks of neuropil-like matrix and cells, and those of

Case 4 were cell clusters scant of neuropil-like matrix. Furthermore, Cases 3 and 4 had an oligoastrocytoma as their glioma component, an unusual participant in the histology of GTNIs. Because of the overlapping histologic features, these cases need to be differentiated from oligodendrogliomas with neurocytic differentiation [13] and malignant gliomas with primitive neuroectodermal tumor-like components [14]. Oligodendrogliomas with neurocytic differentiation are a tumor that has, in addition to typical oligodendrogliomas, small round cells with hyperchromatic nuclei, well-formed Homer Wright-like or perivascular rosettes, and demonstrable neuronal differentiation by immunohistochemistry. The neuronal areas of Cases 3 and 4 did not form Homer Wright-like or perivascular rosettes. Albeit some unusual histologic features for NIs, they showed the basic composition of NIs of GTNI, i.e., the neuropil-like matrix and the cells enmeshed in it. Furthermore, the histologic composition of Cases 3 and 4 is different from that of oligodendrogliomas with neurocytic differentiation. In the former, there were distinct astrocytoma-like areas in addition to distinct oligodendroglioma-like areas, and it was within the astrocytoma-like areas, not in the oligodendroglioma-like areas, that the neuronal areas were present. Whereas in the latter, there are no astrocytoma-like areas, and the neuronal areas are present associated with the oligodendroglioma-like areas [13]. For these reasons, Cases 3 and 4 are differentiated from oligodendrogliomas with neurocytic differentiation. Fluorescence in situ hybridization (FISH) may have been of help for the confirmation of the diagnoses of Cases 3 and 4 since GTNI is expected to be negative for oligodendroglioma-associated chromosomes 1p/19q deletions [12]. We performed FISH for 1p/19q on Case 4, the only case available for the molecular analysis, but the FISH did not yield any positive signals in tumor cells as well as non-neoplastic cells (data not shown).

Malignant glioma with primitive neuroectodermal tumor-like components (MG-PNET) is another tumor from which Cases 3 and 4 need to be differentiated. The PNET-like component of MG-PNET consists of sharply demarcated hyper-cellular nodules with evidence of neuronal differentiation, such as Homer Wright rosettes and the expression of neuronal markers. To be sure, the oligodendroglioma-like areas in Cases 3 and 4 are composed of atypical round cells with hyperchromatic nuclei, but Homer Wright rosettes were absent. Although these areas were weakly positive for Syn, this immunophenotype can also be noted in conventional oligodendrogliomas [15, 16]. Furthermore, the intense immunoreactivity for the mutant IDH1 protein in these areas (Figures 6D, H) preferentially links them to diffuse gliomas [3, 7, 17]. For these reasons, Cases 3 and 4 are differentiated from MG-PNET.

GTNIs with oligodendroglioma-like features have been documented so far. Teo et al. [1] described a case with a subpopulation of small "clear" cells of oligodendrocyte-like morphology. In the series by Barbashina et al. [12], a recurrent tumor in 1 case contained oligodendrocyte-like clear cells that were admixed with a low-grade glioma. The present Cases 3 and 4 are another example showing that GTNIs can have oligodendroglioma-like features.

NIs are essentially identifiable on HE sections without the help of immunohistochemistry. However, there are several markers for NIs. Teo et al. [1] reported uniformly strong labeling for Syn in the matrix of NIs. On the other hand, NFP-immunoreactivity was restricted to differentiated neuronal cells in the perikarya and cell processes. In the present study, Syn-immunoreactivity was strong in all cases (100%). On the other hand, NFP was negative in 3/5 cases (60%). NeuN, which is also a potential marker for NIs [1], was negative in 2/4 cases (50%). The other antigens, including NSE, Olig2, and p53, do not seem contributory as a marker for NIs. Taken together, Syn is likely the most powerful for the labeling for NIs. In addition, it is well known that NIs are constantly negative for GFAP [1], which is also true in the present study. Being positive for Syn as well as being negative for GFAP is the most important immunoprofile of NIs.

What merits mention further about NIs is their proliferative activity. The Ki-67 labeling index (MIB-1 index) of NIs has been reported to be low [1, 18], as it actually was in the present study (Table 2); however, we also encountered a case showing a high MIB-1 index in NIs (Case 5). This is a GTNI with a glioblastoma. A similar case, a GTNI having NIs with a high MIB-1 index (as high as 40%) as well as a glioblastoma, has been re-

ported [11]. Given these 2 cases, the proliferative activity of NIs, at first sight, seems to be determined by the degree of malignancy of the glioma component. However, 1 of the present cases, Case 1, was similarly a GTNI with a glioblastoma; but the MIB-1 index of NIs thereof was conventionally low (Table 2). Conversely, although a case by Keyvani et al. [9] had a diffuse astrocytoma, not a glioblastoma, it showed a relatively high MIB-1 index (mean 3.9%; range 0.6 – 9.3%) in NIs. Given these considerations, the proliferative activity of NIs in GTNI seems independent of the degree of malignancy of the glioma component. What determines the proliferative activity of NIs remains an as yet unsolved, and yet interesting issue to be addressed in the future.

In the present study, 2 out of the 5 cases (40%) showed unequivocal immunoreactivity for IDH1 R132H. The positive cases were GTNIs with anaplastic oligoastrocytoma (Cases 3 and 4). In Case 3, both the Syn-positive area and the GFAP-positive area were positive for IDH1. But interestingly, the IDH1-positive area corresponded to the Syn-positive area rather than the GFAP-positive area in some fields. Another component, the oligodendroglioma-like area, showed the most intense immunoreactivity for IDH1. In Case 4, while neither the Syn-positive area nor the GFAP-positive area was positive for IDH1, the oligodendroglioma-like area was intensely positive for IDH1. The *IDH1* mutation analysis performed on Case 4 showed that both the oligodendroglioma-like area and the astrocytoma-like area had the mutant *IDH1 G395A*. To date, a few studies are available on IDH1 in GTNI [6, 7]. Using a combination of immunohistochemistry and Sequenom-based assay, Huse et al. [6] reported a consistent finding of IDH1 R132H in 9 GTNIs. A recent report from the same group [7] also showed high frequency of IDH1 R132H in GTNIs: a Sequenom-based genotyping analysis combined with immunohistochemistry demonstrated 100% (12 in 12) presence of IDH1 R132H in GTNIs. Studies to date indicate that IDH mutations are largely restricted to diffuse gliomas evolving by way of stepwise malignant evolution, i.e., astrocytomas, oligodendrogliomas, and oligoastrocytomas of WHO GII and GIII or secondary glioblastomas [3, 17]. That Cases 1 and 5 in the present study did not show IDH1-immunoreactivity seems reasonable since these cases were accompanied by primary glioblastomas that are notable for the lack of IDH mutations [3, 17]. The positive percent for IDH1 in the present series (40%) is, accordingly, not inconsistent with the previous reports on IDH1 in GTNI [6, 7]. That the 2 GTNIs with oligoastrocytoma were positive for IDH1 and that the 2 GTNIs with primary glioblastoma were negative for IDH1 seem to be merely following the tumor-specific rule of IDH1 mutations in diffuse gliomas [3, 17]. In this sense, the finding of IDH1 R132H in GTNIs in the present study can be taken as evidence that the tumors are not novel glioneuronal tumors but instead represent conventional gliomas of astrocytic or oligoastrocytic lineage that show aberrant neuronal differentiation.

From the results of immunohistochemistry for IDH1 R132H in Cases 3 and 4, we can gain more insights into IDH1 in GTNI. In Case 3, the Syn-positive areas that were no other than NIs were labeled by the anti-IDH1 R132H antibody. A similar finding was reported by Huse et al. [7], where they documented IDH1 R132H-immunoreactivity in neuronal as well as glial components in all examined cases (7/7 cases). These results indicate that the neuronal component of GTNI can harbor the IDH1 mutation.

In Case 4, the *IDH1* mutation analysis showed that both the oligodendroglioma-like area and the astrocytoma-like area had the mutant *IDH1 G395A*. This result is extremely interesting since the oligodendroglioma-like area was immunohistochemically positive for IDH1 R132H, but the astrocytoma-like area was not. In this case, these two elements constituted distinct areas, and were juxtaposed. This allowed us to sample DNA separately from each element. In a recent paper by Preusser et al. [19], the authors demonstrated that not all tumor cells in a single tumor were immunostained with the anti-IDH1 R132H antibody. They showed a small cell glioblastoma, a diffuse astrocytoma, and an anaplastic gemistocytic astrocytoma in which only a fraction of tumor cells were positive for IDH1 R132H; and yet the three tumors harbored *IDH1 G395A* mutation. In the same report, an anaplastic oligoastrocytoma with biphasic distribution of the two components was shown in which nearly all tumor cells in the oligodendroglial component were positive for IDH1 R132H, whereas in the astroglial component, only a fraction of tumor cells were immunostained; and yet the tumor harbored the

IDH1 G395A mutation. In this study, the genetic analysis of IDH1 status in immunopositive versus immunonegative tumor areas could not be performed. These previous results, in conjunction with ours, suggest that the expression of the mutant IDH1 protein can be regionally heterogeneous even if the mutant *IDH1* gene is ubiquitously present within the tumor. In addition, the result of the *IDH1* mutation analysis on Case 4 suggests that the expression of mutant IDH1 protein can be dependent on each histologic component although the mutant *IDH1* gene is ubiquitously present within the tumor. Some epigenetic mechanism must be operative in the expression of the mutant IDH1 protein, along the way from the gene to the protein, in GTNIs as well as diffuse gliomas.

In conclusion, we have demonstrated diverse pathologic aspects of GTNI spanning its morphology and immunohistochemical features. Also, we have shown that the expression of mutant IDH1 protein in GTNI is largely concordant with that in diffuse gliomas, suggesting the tumor be placed under the spectrum of diffuse gliomas with aberrant neuronal differentiation. Furthermore, we have shown the possibility that the expression of mutant IDH1 protein is dependent on each histologic component although the mutant *IDH1* gene is ubiquitously present within the tumor. These results should prompt further investigations on GTNI or IDH in GTNI.

References

[1] *Teo JG, Gultekin SH, Bilsky M, Gutin P, Rosenblum MK.* A distinctive glioneuronal tumor of the adult cerebrum with neuropil-like (including "rosetted") islands: report of 4 cases. Am J Surg Pathol. 1999; *23:* 502-510.

[2] *Kleihues P, Burger PC, Rosenblum MK, Paulus W, Scheithauer BW.* Anaplastic astrocytoma. In: Louis DN, Ohgaki H, Wiestler OD, Cavenee WK (eds). WHO classification of tumours of the central nervous system. Lyon: IARC; 2007. p. 30-32.

[3] *Yan H, Parsons DW, Jin G, McLendon R, Rasheed BA, Yuan W, Kos I, Batinic-Haberle I, Jones S, Riggins GJ, Friedman H, Friedman A, Reardon D, Herndon J, Kinzler KW, Velculescu VE, Vogelstein B, Bigner DD.* IDH1 and IDH2 mutations in gliomas. N Engl J Med. 2009; *360:* 765-773.

[4] *Riemenschneider MJ, Jeuken JW, Wesseling P, Reifenberger G.* Molecular diagnostics of gliomas: state of the art. Acta Neuropathol. 2010; *120:* 567-584.

[5] *Watanabe T, Nobusawa S, Kleihues P, Ohgaki H.* IDH1 mutations are early events in the development of astrocytomas and oligodendrogliomas. Am J Pathol. 2009; *174:* 1149-1153.

[6] *Huse J, Nafa K, Ladanyi M, Hedvat C, Rosenblum M.* Glioneuronal tumor with neuropil-like islands (GTNI) is characterized by IDH1 R132H mutations [abstract 108]. J Neuropathol Exp Neurol. 2011; *70:* 526-527.

[7] *Huse JT, Nafa K, Shukla N, Kastenhuber ER, Lavi E, Hedvat CV, Ladanyi M, Rosenblum MK.* High frequency of IDH-1 mutation links glioneuronal tumors with neuropil-like islands to diffuse astrocytomas. Acta Neuropathol. 2011. in press.

[8] *Ohgaki H, Dessen P, Jourde B, Horstmann S, Nishikawa T, Di Patre PL, Burkhard C, Schüler D, Probst-Hensch NM, Maiorka PC, Baeza N, Pisani P, Yonekawa Y, Yasargil MG, Lütolf UM, Kleihues P.* Genetic pathways to glioblastoma: a population-based study. Cancer Res. 2004; *64:* 6892-6899.

[9] *Keyvani K, Rickert CH, von Wild K, Paulus W.* Rosetted glioneuronal tumor: a case with proliferating neuronal nodules. Acta Neuropathol. 2001; *101:* 525-528.

[10] *Prayson RA, Abramovich CM.* Glioneuronal tumor with neuropil-like islands. Hum Pathol. 2000; *31:* 1435-1438.

[11] *Vajtai I, Reinert MM.* Malignant glioneuronal tumor of the adult cerebrum with neuropil-like islands involving "proliferating nodules": confirmatory report of an unusual variant. Acta Neuropathol. 2007; *113:* 711-713.

[12] *Barbashina V, Salazar P, Ladanyi M, Rosenblum MK, Edgar MA.* Glioneuronal tumor with neuropil-like islands (GTNI): a report of 8 cases with chromosome 1p/19q deletion analysis. Am J Surg Pathol. 2007; *31:* 1196-1202.

[13] *Perry A, Scheithauer BW, Macaulay RJB, Raffel C, Roth KA, Kros JM.* Oligodendrogliomas with neurocytic differentiation. A report of 4 cases with diagnostic and histogenetic implications. J Neuropathol Exp Neurol. 2002; *61:* 947-955.

[14] *Perry A, Miller CR, Gujrati M, Scheithauer BW, Zambrano SC, Jost SC, Raghavan R, Qian J, Cochran EJ, Huse JT, Holland EC, Burger PC, Rosenblum MK.* Malignant gliomas with primitive neuroectodermal tumor-like components: a clinicopathologic and genetic study of 53 cases. Brain Pathol. 2009; *19:* 81-90.

[15] *Koperek O, Gelpi E, Birner P, Haberler C, Budka H, Hainfellner JA.* Value and limits of immunohistochemistry in differential diagnosis of clear cell primary brain tumors. Acta Neuropathol. 2004; *108:* 24-30.

[16] *Wharton SB, Chan KK, Hamilton FA, Anderson JR.* Expression of neuronal markers in oligodendrogliomas: an immunohistochemical study. Neuropathol Appl Neurobiol. 1998; *24:* 302-308.

[17] *Balss J, Meyer J, Mueller W, Korshunov A, Hartmann C, von Deimling A.* Analysis of the IDH1 codon 132 mutation in brain tumors. Acta Neuropathol. 2008; *116:* 597-602.

[18] *Allende DS, Prayson RA.* The expanding family of glioneuronal tumors. Adv Anat Pathol. 2009; *16:* 33-39.

[19] *Preusser M, Wöhrer A, Stary S, Höftberger R, Streubel B, Hainfellner JA.* Value and limitations of immunohistochemistry and gene sequencing for detection of the *IDH1-R132H* mutation in diffuse glioma biopsy specimens. J Neuropathol Exp Neurol. 2011; *70:* 715-723.

Cancer Science
The official journal of the Japanese Cancer Association JCA

Significance of *IDH* mutations varies with tumor histology, grade, and genetics in Japanese glioma patients

Akitake Mukasa,[1,9] Shunsaku Takayanagi,[1] Kuniaki Saito,[1] Junji Shibahara,[2] Yusuke Tabei,[3] Kazuhide Furuya,[4] Takafumi Ide,[5] Yoshitaka Narita,[6] Ryo Nishikawa,[7] Keisuke Ueki[8] and Nobuhito Saito[1]

Departments of [1]Neurosurgery, [2]Pathology, University of Tokyo, Tokyo; [3]Department of Neurosurgery, Tokyo Metropolitan Cancer and Infectious Diseases Center Komagome Hospital, Tokyo; [4]Department of Neurosurgery, Teikyo University School of Medicine, Tokyo; [5]Department of Neurosurgery, Tokyo Metropolitan Bokutoh Hospital, Tokyo; [6]Department of Neurosurgery and Neuro-Oncology, National Cancer Center Hospital, Tokyo; [7]Department of Neuro-Oncology/Neurosurgery, International Medical Center, Saitama Medical University, Saitama; [8]Department of Neurosurgery, Dokkyo University School of Medicine, Tochigi, Japan

(Received October 20, 2011/Revised November 24, 2011/Accepted November 29, 2011/Accepted manuscript online December 2, 2011/Article first published online January 13, 2012)

Mutations in isocitrate dehydrogenase 1 (*IDH1*) and *IDH2* are found frequently in malignant gliomas and are likely involved in early gliomagenesis. To understand the prevalence of these mutations and their relationship to other genetic alterations and impact on prognosis for Japanese glioma patients, we analyzed 250 glioma cases. Mutations of *IDH1* and *IDH2* were found in 73 (29%) and 2 (1%) cases, respectively. All detected mutations were heterozygous, and most mutations were an Arg132His (G395A) substitution. *IDH* mutations were frequent in oligodendroglial tumors (37/52, 71%) and diffuse astrocytomas (17/29, 59%), and were less frequent in anaplastic astrocytomas (8/29, 28%) and glioblastomas (13/125, 10%). The pilocytic astrocytomas and gangliogliomas did not have either mutation. Notably, 28 of 30 oligodendroglial tumors harboring the 1p/19q co-deletion also had an *IDH* mutation, and these alterations were significantly correlated ($P < 0.001$). The association between *TP53* and *IDH* mutation was significant in diffuse astrocytomas ($P = 0.0018$). *MGMT* promoter methylation was significantly associated with *IDH* mutation in grade 2 ($P < 0.001$) and grade 3 ($P = 0.02$) gliomas. *IDH* mutation and 1p/19q co-deletion were independent favorable prognostic factors for patients with grade 3 gliomas. For patients with grade 3 gliomas and without 1p/19q co-deletion, *IDH* mutation was strongly associated with increased progression-free survival ($P < 0.0001$) and overall survival ($P < 0.0001$), but no such marked correlation was observed with grade 2 gliomas or glioblastomas. Therefore, *IDH* mutation would be most useful when assessing prognosis of patients with grade 3 glioma with intact 1p/19q; anaplastic astrocytomas account for most of these grade 3 gliomas. (*Cancer Sci* 2012; 103: 587–592)

Gliomas are among the most common and formidable brain tumors.[1] Despite intensive treatment, most patients die within 2-10 years. Therefore, development of novel therapeutic strategies based on greater understanding of tumor characteristics is needed. Recently, a comprehensive sequence analysis of human GBM that included most human genes revealed frequent mutations in *IDH1*.[2] Subsequent analyses revealed that these mutations occur more frequently in low-grade glioma than in GBM, with a rate of *IDH1* mutation as high as 59–90%.[3–7] The *IDH* gene mutation is currently believed to occur in the early stage of gliomagenesis[4,6] and to play a critical role in tumor development.

The *IDH* genes encode redox enzymes; these enzymes convert isocitrate to alpha-ketoglutarate, use NAD(P)+ as a coenzyme, and function in energy metabolism. There are three *IDH* genes in humans, and only mutations in *IDH1* are frequently found in gliomas; the IDH1 enzyme resides in the cytosol and peroxisomes.[2,7] Mutations in *IDH2* are rare in gliomas; IDH2 localizes to mitochondria and functions in the Krebs (citric acid) cycle. To date, no *IDH3* mutation has been reported. Most *IDH1* mutations in gliomas are missense mutations at amino acid 132, which is in the catalytic domain and binds to substrate. Similarly, *IDH2* mutations in gliomas are substitutions at amino acid 172, which is functionally equivalent to amino acid 132 of IDH1. *IDH1* and *IDH2* mutations in the catalytic domain are also found in 8–23% of acute myeloid leukemias.[8,9] Mutations in *IDH* genes are rarely found in other tumors.[7,10]

In general, a tumor with an *IDH* mutation has either an *IDH1* or *IDH2* mutation, and the mutation is heterozygous with a wild-type allele.[2,4,6,7] This observation led to the notion that mutated *IDH1/IDH2* genes gain novel functions and are oncogenes, and that the wild-type *IDH* genes are not tumor suppressor genes. In fact, mutant IDH1 has novel enzymatic activity; it converts alpha-ketoglutarate to 2-HG, and accumulated 2-HG is presumed to contribute to tumorigenesis as an "oncometabolite".[9,11–13]

Malignant gliomas categorized as WHO grade 4[2,5,7,14,15] or grade 3[5,7,15–17] with an *IDH* mutation were reportedly associated with higher PFS[15–17] and OS[2,5,7,14–17] than those without an *IDH* mutation. However, for grade 2 gliomas, the relation between the presence of an *IDH* mutation and prognosis is controversial.[15,18–20]

The *IDH* mutations apparently have an important role in many aspects of glioma, including gliomagenesis, patient prognosis, and development of therapeutic strategies. However, information on *IDH* mutations in gliomas, such as prevalence, relation to other genetic alterations, and prognostic value, is still limited, particularly for Asian populations,[21,22] including Japanese patients.[5,17] Thus, to further clarify the significance of *IDH* mutations with regard to proper diagnosis and optimized treatment of malignant gliomas, we sought basic data on a large number of Japanese glioma patients for *IDH1* and *IDH2* mutations and other genetic and epigenetic alterations frequently found in gliomas, specifically 1p/19q LOH, *TP53* mutation, and *MGMT* promoter methylation.

Materials and Methods

Tumor specimens. Tumor samples and paired blood samples were obtained following surgery. Of 250 gliomas, 168 tumors were collected at the University of Tokyo hospital (Tokyo,

[9]To whom correspondence should be addressed.
E-mail: mukasa-nsu@umin.ac.jp

doi: 10.1111/j.1349-7006.2011.02175.x